Università degli Studi di Roma “Tor Vergata”

Dipartimento di Ingegneria Meccanica

Dottorato di Ricerca in Ingegneria dei Microsistemi

XVII Cycle

CHARACTERIZATION OF PIEZORESISTIVE PROPERTIES IN CVD DIAMOND FILMS TO BE USED AS STRAIN GAUGE

Candidate

Ing. Gonzalo Rodríguez

Coordinator

Prof. Aldo Tucciarone

Tutor

Prof. Aldo Tucciarone

Acknowledgements

In first place I want to acknowledge and to be thankful to my Family and Maria Laura, my Fiancée and future Wife, for all the support, patience, push and love with which have accompanied me in this demanding period of my life. Without your support I couldn't never have succeed; for all of you my love, admiration and eternal gratitude.

I also want to gratefully acknowledge Prof. Antonio Paoletti, Prof. Aldo Tucciarone, Prof. Enrico Milani, Prof. Marco Marinelli, Dr. Gianluca Verona Rinati and my doctorate companions Gianluca Pucella and Antonio Balducci for introducing me in microsystems field, in particular regarding the physics of diamond and their possible applications, and for their patient tutoring and support in developing my research activities. Moreover, I want to gratefully acknowledge my companions for their critical analysis in writing the present work. At this point I want to underline the tutoring in experimental activities in the laboratory and their theoretical continuously support essential in the development of this thesis work. I also want to emphasize and to thanks for helping me in the growth that I have had like person and professional in these three years.

At the end a special thanks for all the person that have been near me inside or outside the university in this PhD period in a foreign country; this work is also for you.

“Si pude ver más lejos es porque estoy parado sobre hombros de gigantes”

“If I could see further is because I’m standing over giants’ shoulders”

Isaac Newton

A mis Padres: “Ustedes son mis Gigantes”

To my parents: “You are my Giants”

Contents

Chapter 3 Growth and characterization of boron – doped CVD diamond films

Chapter 4 Piezoresistive effect in boron – doped CVD diamond films

Chapter 5 Experimental setup of piezoresistive effect demonstrator

Chapter 6 Time response of boron – doped CVD diamond films

Chapter 7 Experimental results of piezoresistive measurements

INTRODUCTION

The increasing exigency of more automated and easier to use devices suppose the fabrication of systems able to measure some physical or chemical quantities and to react in consequence automatically, operating, then, in a partially autonomous way. For this particular interest, in the last years, big efforts were made in order to develop Microsystems. With "Microsystems" we intend a miniaturized system made of one or more sensors that put in evidence and measure physical and chemical magnitudes, producing a signal that is opportunely processed and used for accomplishing a well established electrical, optical, chemical or mechanical function.

Microsystems could be considered as a result of the integration methodologies and technologies belonging to mechanics, electronics and informatics, joined in design and construction steps allowing the realization of cheapest, simplest, more reliable and more flexible devices. The possibility of integrating mechanical and electronic components in the same device has established a radical change in the project philosophy of a large number of products. For this reason, microsystem technologies represent the methodological and technical support that better characterize high number of sectors technologically advanced (i.e.: Autronics, industrial automation, consumer electronics, mobile communications and health).

Current microsystem technology is related almost exclusively to silicon. This material presents very important electronic characteristics besides its good mechanical properties. Moreover, the use of silicon in microelectronics has established an important knowledge of this material and related technologies. Then, the base technologies for the realization of microsystems are those developed for the manufacturing of integrated circuits based on silicon., it means, lithography, chemical attacks and film growing. These

technologies afterwards allowed the development of specific microsystems technologies, derived from precision mechanics and other sectors as physics.

However, there are limits to mechanical, thermal and electrical properties of silicon for specific applications in which the capability to operate at high temperature and to resist high radiation flux or chemical attacks is important. In order to compare the new technological challenges in the realization of devices for novel applications, research and development of new materials are needed. *Diamond* and in particular *polycrystalline diamond*, produced with *CVD (Chemical Vapor Deposition)* technique, is without any doubt an outstanding material in its mechanical, optical, thermal and electronic properties, that makes it very interest for different applications. Moreover, due to the high bandgap between valence band and conduction band (apt to operate at high temperatures or in presence of light) and because of its outstanding physical and electronic properties, as it high fusion point, its low chemical reactivity and it extreme robustness, diamond seems to be a natural candidate to be used in harsh/hostile environment. Obviously, in order to take advantage of all its possible applications it is important to have good quality diamond, thus it is mandatory the study of diamond physical properties, with the goal of better understand its characteristics at high temperature that constitutes a harsh environment.

In this context is placed the present PhD thesis. It is centered on the study of diamond doping and piezoresistive effect on boron doped p-type diamond grown at the Mechanical Engineering Department of the University of Rome “Tor Vergata” laboratories. This work also presents a study of the mentioned effect at high temperature in order to establish some parameters that must be taken into account for the realization of potential strain gauge apt to be used at high temperature.

In particular, this work is developed in seven chapters. In the first one there is an introduction to microsystems, with references to the advantages that offer and the different

possible applications. Later the main fabrication techniques are presented, beginning from those derived from microelectronics to that specific of microsystems. In the second chapter diamond properties are analyzed, focusing on that properties that make diamond an outstanding material for the realization of microsystems apt to be used in harsh/hostile environments. Also in the second chapter, main synthesis processes of artificial diamond are analyzed, among them plasma enhanced *CVD* technique, that is the one used at the Mechanical Engineering Department of the University of Rome "Tor Vergata" laboratories for the growth of diamond film.

In the third chapter it is described the growth and Boron doping process that lead to obtain p-type doped diamond samples, it is described in detail the necessary equipment, the growth conditions and the parameters that must be taken into account in order to manage a doping growth. It is also described the theory behind the experimental facts, especially described that of conduction mechanisms in doped diamond; characterization through R(T) and experimental results are shown. Always in third chapter *Temperature Coefficient of Resistance* (TCR) will be defined and calculated and evaluated its behavior with different doping levels, we will also see its importance in future measurements due to its capability of hiding piezoresistive effect. Moreover, systematic studies of the chamber dynamics is also presented, both with methanol in the growth chamber and without it, it is notice that methanol content act as an inhibitor in doping efficiency, because of its oxygen content that combine the residual boron (in the chamber) to produce boron oxide (B_2O_3).

The fourth chapter describes the theory of piezoresistive effect that is the main effect analyzed in this work. First of all, it is described the main response parameters affecting the operation of any sensor device that are sensor response curve, internal sensitivity and resolution, noise and drift. Moreover a numerical approach to piezoresistive effect is presented, that gives the reader a self-content description of the main parameters

involved in piezoresistive effect; after that, some motivations are presented to give the reader the whole picture in which Boron-doped diamond based strain gauge could be used.

The last three chapters are dedicated to the main application of this PhD work that is the development of a demonstrator able to show the mentioned effect and the potentiality for making diamond based strain gauges. In particular the fifth chapter is intended to describe the experimental setup of the demonstrator apparatus, in which it is explained its construction, its functionality, the force application system and its thermal regulation, moreover, diagrams and pictures are also presented in order to enlighten how it works and what we can expect from measurements. Later in the sixth chapter, time response of diamond samples is analyzed; this chapter has two main scopes, the first is investigate the time response as a function of different parameters that could be real work conditions of a potential strain gauge (i.e.: temperature, strain, doping level). The other scope is to established the pause needed for the sample to reach the steady state when voltage is varying, that is, in order to make *I-V* measurements voltage must be varied (through a programmable voltage source) then a pause must be done in order to allow diamond to stabilized and then make data acquisition. In the last chapter, the main results of piezoresistive effect on diamond samples grown at the Mechanical Engineering Department of the University of Rome "Tor Vergata" laboratories are presented, *I-V* characteristic were performed in order to study the electrical behavior of diamond samples; relative change of resistance ($\Delta R/R$) and *gauge factor* (GF) are presented as a function of doping level and applied strain; moreover, in order to analyze diamond behavior at high temperature, measurements were made, in which, we will see the capability of diamond as sensing material apt to be used in harsh environments. Studies of the variation of $\Delta R/R$ and GF with doping level will enlighten potential application of diamond as a strain gauge.

Chapter 1

The Microsystems

Summary

The development of microelectronics technologies and their integration with mechanical, optical, chemical or biological systems have made grow, specially in the last decade, the interest in *microsystems*, it means miniaturized systems composed by sensors which measure a physical or chemical magnitude then converting this measure in an electrical signal. This signal is properly elaborated through integrated electronics in the same sensor and sent to an actuator who performs the desired command.
The use of microsystems offer interesting advantages: more functionality and reliability, less power consumption, little dimensions and weight, low cost and flexibility in design and production stages. However, mass production, at the moment, is only available for a few numbers of sectors of interest, i.e. autronics, industrial automation, consumer electronics, mobile communications and biomedicine.
The most useful material for microsystems production is the silicon, because of their good mechanical and electronic properties, that allowed all the production technologies from the microelectronics to be used, with other specific technologies developed ad-hoc from precision mechanics and physics, in microsystems production.

1.1 THE MICROSYSTEMS

The possibility of integrating microelectronics technologies with mechanical, optical, chemical or biological systems in miniaturized structures, supporting by the exigency of obtaining high functional complexity and very low dimensions devices, has made develop, in the last years, a particular interest to the *microsystems*.

The term *microsystem* indicates a miniaturized system composed of *sensors* which measure chemical and physical magnitudes then converting such magnitudes in an electrical signal, an integrated circuit with *analyzer* functions of signal processing and one or more *actuators* with the received command from the analyzer execute different actions to the external environment [1,2]. The general scheme of a microsystem is illustrated in Fig 1.1.

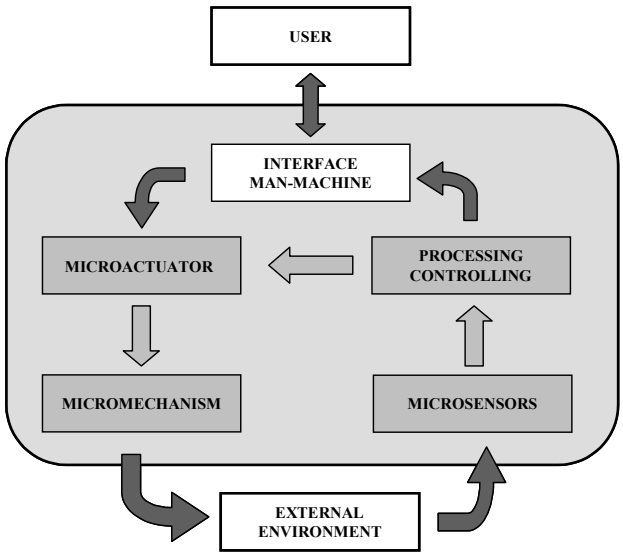

Fig. 1.1 General scheme of a microsystem.

Microsystems can be considered derivatives from the complementary use, at miniaturized level, of electronic, mechanical, optical, biological and informatics technologies, for which one of the fundamental characteristic is the multidisciplinary knowledge that is needed in order to develop a device.

It's clear that the degree of "intelligence" of a microsystem is higher as higher is the capability of interacting, autonomously with the surrounding environment, in an fast and efficiency way due to the integration of a number always higher of sensors, processors and actuators. That explains the miniaturization trend always find in microsystems, an analogous thing happens in microelectronics, with the noted complication of the microsystem integration with electric, optical, mechanical and chemical functions.

1.2 APPLICATIONS AND ADVANTAGES OF MICROSYSTEMS

The use of microsystems offers a very interesting series of advantages from a point of view of application: higher functionality, due to the electric and non-electric functions integration in very low spaces; higher reliability, due to the high integration between components; low power consumption, low weight and dimensions, low cost and high flexibility in project and production stages.

The microsystems are recently incorporated in the industrial production frame in order to satisfy different needs in a wide spectra application [3-5]. So, mass production is at the moment for a few industrial production sectors, such as, autronics, industrial automation, consumer electronics, mobile communications and biomedicine.

The *autronics* represent without a doubt the highest production volume and in which microsystems find the highest number of applications (historically is the field in which were first applied as exhaust gas microsensors in catalyzed systems in vehicles). It was anticipated that in a few years sensors and electronic components will represent approximately the 30% of the value of a car, moreover, the present applications are in a very wide range: accelerometers, pressure sensors, temperature, air and carburant flows, exhaust gas, are nowadays integral part of a modern car.

Combustion chamber and tires control systems are needed to be solved with microsystems, are also needed in exhaust catalyzed systems, ABS (Anti-lock Braking System), Anti-slide system, active damping system, airbag protection system for passengers, all of these systems widely use pressure sensors for its operation.

In the field of *industrial automation* microsystems are fundamental in robotics and in fields incompatible with human intervention. In this market area will be highly required in near future products such as: pressure sensors, accelerometers, flow sensors, structural damage monitors and chemical sensors apt to measure specific concentration of chemical species.

Consumer electronics and mobile communications with miniaturized transmission systems, recording and reproduction data systems, high definition visualization and printing systems are able fields to absorb high production volumes.

Another development microsystems area is represented by *biomedicine*, where microsystems could completely revolutionize this application field.
At the moment microsystems are highly necessary for artificial organs control, microsurgery, auditory support advice, stimulation of implanted nerves and recently for liquid analysis and drug automatic and intelligent provision control systems (i.e.: insulin for diabetics). It's clear that a point of fundamental importance is the biocompatibility for which is a main role the R&D in new materials.

An area which is believed to have a strong expansion, with a strong industrial stimulus because of commercial possibilities is the *domotics*. In this field microsystems will allow more comfortable, cheaper and highly safer all the activities in domestic environment thanks to automation systems (i.e.: selective sensors of temperature, humidity, pH control), gas flow and liquids control devices, security sensors for identification of gas presence (i.e.: carbon monoxide or methane).

Microsystems will be able to contribute essentially in *environment control*: they will contribute in different ways to environmental protection, through miniaturized systems for water and air monitoring (chemical sensors), the study of chemical and physical properties of used substances, analysis and control of emissions (for vehicles and rooms) and monitoring of contamination by environmental radiation.

Agriculture, at the end, will be in conditions of taking advantages from devices which will be able to do land control from nutritious and polluting agents, maturation degree and possible presences of diseases in vegetal products (from appearance of individual diseases or epidemical ones), moreover, production related controls and quality in industrial treatment of foods.

We close this paragraph reporting in Fig 1.2 an idea of the dimension of the microsystem market in the United States related to the three greater sectors in volume production [6].

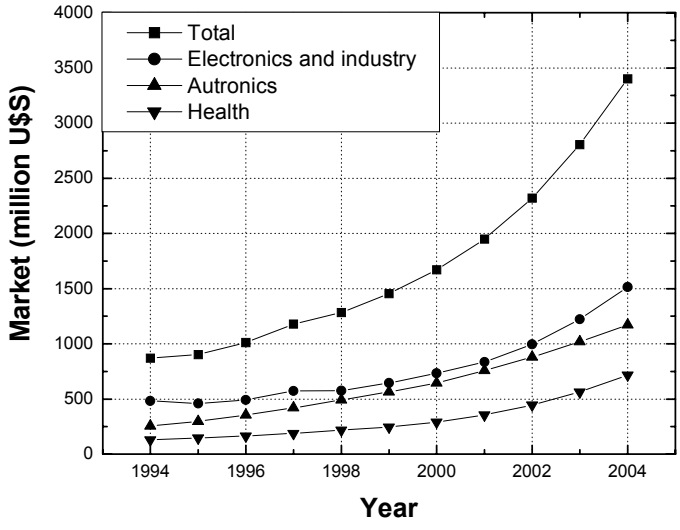

Fig. 1.2 Analysis and forecast of microsystems in the United States market.

1.3 MICROSYSTEM MANUFACTURE

The material mainly used in microsystem manufacture is silicon, which besides being an optimal semiconductor presents satisfactory mechanical properties [7]. In addition, the good knowledge of this material, acquired in microelectronics development, allows the use in microsystem production of all manufactures technologies typical from microelectronics, for example lithography, chemical attack and film growing. The use of silicon guarantees the best possible integration between mechanical and electric components, for which, it's possible to produce in a silicon substrate micromechanical devices and integrate, on the same substrate, control electronics.

However, it's important to underline that for microsystems production, besides using all typical technologies from microelectronics, is necessary to use some other technologies specific of microsystem derived from precision mechanics (microstereolitography) or some from another area such as physics (laser micromachining, LIGA technique). In fact, traditional techniques for manufacture and working of silicon microstructures are not always sufficient for the manufacture of microelectromechanical devices, because they are essentially planar type techniques which doesn't allow the manufacture of really three-dimensional structures for mechanical and electronic functions.

In Fig. 1.3 is shown a general scheme of microsystem manufacture, which has mainly three phases: a phase of deposition, one of lithography and another one of material removal.

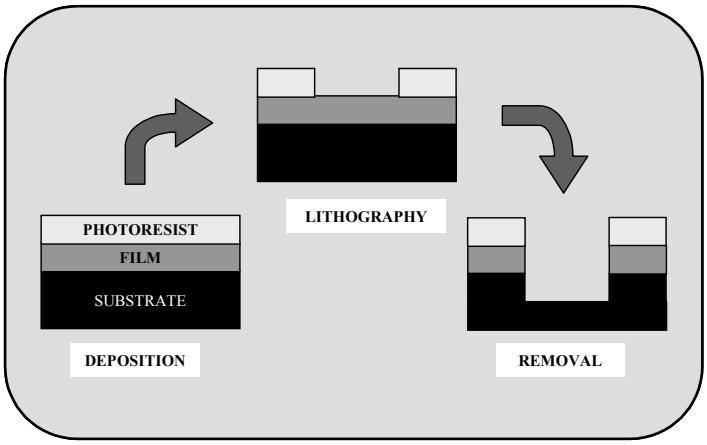

Fig. 1.3 Base process in microsystem elaboration: Material layer are deposited, the pattern is transferred onto the photoresist then removal of surface and bulk material. The process is repeated till complete the desired microstructure.

In particular, the three phases are repeated until completing the microstructure. Let us analyze separately the three phases of a microsystem manufacture.

1.4 DEPOSITION TECHNIQUES

The traditional technology for electronic microdevices manufacturing is based on the deposition and microelaboration of silicon substrates, dielectrics (ex: SiO_2) and metals (typically Al, but Ag and Au too). So, for the deposition of any device is essential to have the possibility of depositing substrates of this materials. Let us consider some of the more diffuse techniques for the elaboration of metallic layers and dielectric layers, noticing that the use of a particular technique instead another strongly depends on the kind of layer that has to be done [8].

The most common process for contact deposition and different metallic layers deposition is the *thermal evaporation*, which is based on the vacuum evaporation of the material to deposit.

The substrate on which it is wanted to deposit the material is placed near the evaporation source, which is heated with a thermal heater or through an electron beam. This technique allows obtaining high quality and a high directionality of the deposited layer.

The *Chemical Vapor Deposition* (CVD) is the most used technique for depositing silicon oxide, because it produces high isotropic layers avoiding problems of "shades" still in presence of cavities and complex morphologies and because allows, quickly, depositing large areas. The CVD is essentially based on the "reaction" of some gases in a high temperature chamber (400 / 600 °C); in individual, one of the reaction products is the compound that is wanted to be produced which is deposited on a wafer who acts as the substrate. The system is mainly constituted of a furnace that is filled and regulated with the necessary gases. For example, silicon oxide is deposited through the following reaction:

$$SiH_4 + O_2 \rightarrow SiO_2 + 2H_2$$

Polycrystalline silicon can also be produced taking advantage of the CVD technique; in this case the system operates in a range of temperature between 600 – 650 °C and it is verified a reaction of molecular division of the SiH_4 induced by thermal agitation:

$$SiH_4 \rightarrow Si + 2H_2.$$

The *sputtering* indicates the technique based on the production of ions of the material to deposit by effect of inert ion collisions opportunely accelerated (generally Argon ions) against the surface of the material to deposit [9,10]. A general scheme for a sputtering apparatus is essentially composed of two electrodes between which it is applied a potential difference; the material to deposit is normally positioned on the cathode, the Ar ions, produce at low pressure and temperature through electrical discharges or radio frequency, are accelerated by the potential difference and hit the material to deposit causing the cession of atoms which fill the substrate to cover.

1.5 LITHOGRAPHIC METHOD

Once deposited a layer on the substrate the next step is the microsystem realization, that consists of covering the layer with a photosensitive substance (resist) and "design" on the resist the structure (pattern) of the object to be produced on the substrate. The main technique used to transfer the pattern in the resist is the lithography; this technique consists of making a mask on which the structure is transferred to make in the resist. In this point the mask is illuminated through an opportune radioactive source and thus resist comes made an impression from the image of the pattern. In the other hand, the pattern must be transferred on the substrate, for which, at we will see, the lithographic process is followed of a process of removal of the parts no masked, that removal could be accomplished by chemical attack techniques, plasma techniques or optical techniques (laser) [11]. In the removal process the non-impressed resist is used as a protective mask against the removal of the material below.

The lithographic process could be done in different ways depending on the type of radiation used.

In the *optical lithography* ultraviolet radiation (200 – 400 nm) is used, the transfer of the pattern to the mask could be done putting the mask in contact (or almost in contact) with the photoresist (*contact and proximity printing*), or through projection techniques. In the case of contact printing resolutions of the order of the micron could be reached but it's possible to have a mask damage due to the physical contact with the photoresist; it's why proximity printing is safer, because physical contact between mask and photoresist is avoided, in the other hand, resolution is lower (2 – 5 μm).

At the end, in the projection method the mask damage is limited because the substrate is placed at several centimeters from the mask, and the worsening of the resolution due to the diffusion of the radiation could be compensated using a bigger dimension mask, because in

projection phase the dimension of the object projected could be reduced, that allows to obtain resolutions similar to the contact lithography.

The X-ray lithography [12,13] is similar to the optic one, in particular, to use X-ray (RX) allows obtaining very high resolutions (till 0.1 μm) and producing deeper structures. The main difficulty in using RX is the physical duration of the mask, being impossible to use projection techniques.

In the *electron beam lithography* [11] the resist is printed by an electron beam electronically controlled for which is not necessary the mask for pattern transfer. This technique offers, in principle, a greater resolution with respect to optical lithography, because the wavelength of an electron beam of energies of 20 – 50 keV is inferior to1 nm. In fact, resolution limit, in this type of lithography, is established by other factors, for ex: electron scattering inside the material below the resist (because of this electrons can print zones next to the one of interest), the aberration of the electrical and magnetic lenses used to focus the beam on the interest area, the magnetic interaction between electrons of the beam, resist properties, etc. This effect limits the resolution to 200 – 300 nm approximately, in order to diminish the resolution below 200 nm it is necessary to use an ion beam (that as is known they present lower ranges and more linear trajectories in the matter that the electrons), but of more complex use.

1.6 REMOVAL METHODS

Once finished the process of lithographic reproduction of the structure of the object to make, starts the true and the own one “mechanical” elaboration, in order to transfer the pattern from the resist to the substrate; the more used methods in this step are the *etching* and the *laser micromachining*.

1.6.1 Etching

Almost all lithographic processes use for micro-elaboration the as known etching, which is in practice the removal of the unprotected parts from the resist, with the objective to obtain the desired structure on the substrate. In particular, there are different types of etching.

The *chemical etching* [14] or *wet etching*, it's a "chemical" attack method from reagents in liquid solution that previews two steps: in the first step it is performed an oxidation process of the surface through oxidizing agents such as nitric acid (HNO_3), this step is followed by the step of dissolution of oxide through a proper dissolvent (HF, CH_3COOH). In particular, on the base of the technique of *bulk micromachining* are the principles of the anisotropic chemical attack, which is based in the properties of some chemical agents of different attack speed related to the crystallographic orientation from the material to be attacked (for ex: there is a 100 factor in the attack speed of the KOH for (100) and (111) planes of the silicon): taking advantage of this property it is possible to produce well defined structures. It is opportune to remember that most of the materials present a polycrystalline structure, so, for this materials the chemical attack is mainly isotropic and inevitably will be attacked under the resist profile giving rise to *undercutting* effects, it means the non-desired part removal of the material; therefore this etching type is not adapted to high spatial resolution elaboration (in general the obtained resolution is in the order of the thickness of the layer to be attacked) and for very deep attacks.

An etching that is distinguished for his enunciated anisotropy is the *plasma assisted etching* [14,15] or *dry etching*, which is a "mechanical" etching that consists mainly in the ion-surface interaction which allows to remove the non-desired material. In particular, one of the used techniques is that of the "*back sputtering*" and is in practice the reverse one of the *sputtering*. In this case the substrate with the material to be removed is placed on the

cathode, where the accelerated argon ions produce the sputtering reaction removing the non-desired material. As it was told, the advantage of this kind of etching is essentially the possibility of making highly anisotropic etching, due to the fact that all reactions are made in preferential way in the orthogonal direction of the substrate.

1.6.2 Laser micromachining

Between the microelaboration techniques, one of most diffuse is the *laser micromachining*, which belongs to the family of the elaboration by material removal. In particular, this technique, which can be used for different materials, consists in the material removal through the focalization of a laser beam. It is important to notice that it is a thermal process and the material is removed by fusion and evaporation, for which the excessive heating can damage the surrounding zones to the radiated one.

In order to solve this kind of problems and to improve the resolution of the elaboration, it is developed gradually the *excimer laser microlithography* [16], in which is used a laser that emits photons between 130 and 350 nm. This technique is in principle similar to the traditional optical technique, nevertheless presents some advantages mainly referred to the type of physical interaction between the laser beam and the photoresist. In fact, because of the high energy density of the laser beam, this is in degree of breaking the molecular unions from the molecules directly exposed to the radiation, creating a fast dissociation and a fast expulsion of the material by ablation, but without attacking adjacent molecules. This fact allows to obtain much more defined contours and to reduce the exposed surface to a strong heating, then avoiding the damage of the surrounding zones to the radiated one. In particular, the transfer of the pattern could be done using a mask, generally made of an amorphous quartz substrate (SiO_2) covered with chromium layers (this type of mask doesn't allow to obtain inferior structures to 130 nm, because for

smaller wavelength they do not transmit the radiation), which directly, varying the speed of the sample with respect to the laser, the intensity of employed energy and the number of hits in every point, allows to obtain by this way very complex structures.

1.7 ADVANCED ELABORATION METHODS

Between the technologies of advanced type, arisen from the necessity to make three-dimensional structures for the manufacture of microsystems, the most used is without a doubt the *LIGA* [17] (*Lithographie Galvanoformung Abformung*). The LIGA is a manufacture technique based on a combination of X-ray lithography, with deep material attack, electric mold preparation and stamping. In particular, the structure is made exposing to the RX, through a mask, a photosensitive polymer layer (such as polymethyl meth-acrylate, PMMA) placed on a substrate. At this point, after removal the exposed parts through washing in an opportune chemical solution, it is possible to proceed to the galvanic electro deposition of a metallic layer (generally made of nickel), which represents, once removed the remaining polymer and the substrate, a stamp of the wished object, which can be used directly for printing processes. Obviously, for more complex three-dimensional structures, at different levels, it can be repeated all the listed processes with another mask. The LIGA applications are always expanding to the possibilities of obtaining deep and precise elaborations in variable thicknesses and because with LIGA can be obtained prints of the wished object which can be used several times, making by this way the object in series.

Nevertheless, the technique who best allows the elaboration of complex three-dimensional geometries is the *microstereolitography* [18], which operation principle is very simple; in practice, a pattern generator, typically constituted of a transparent liquid

crystal screen, generates the design of each single part of the structure to be done; the image of each part is then focused, through a radiation source, on the surface of a liquid photopolimerizable resin (contained in a suitable container), that solidifies in the radiated region. Obtained the first step, the sample is immersed in the resin so that a new liquid resin layer covers the cured layer and the new structure of the second part is reproduced as the previous case and so on till accomplished the elaboration of each single step of the desired microstructure.

Chapter 2

The Diamond

Summary

The use of silicon as base material for the elaboration of microsystems is not in degree to satisfy all possible applications of microsystems, specially those that are in hostile environments of several types. Research and development in new materials for the microsystems elaboration result then an important part of the work in the microsystems field. In particular, diamond is a material that has exceptional mechanical, optical, thermal and electronic properties that they render it specially apt for harsh environments. Between the different production techniques from artificial diamond, the *CVD (Chemical Vapor Deposition)* plasma enhanced technique is characterized by the high purity of obtained films and is then particularly interesting for the production of microsystems. At the laboratories of the Mechanical Engineer Department of the University of Rome "Tor Vergata" are deposited CVD diamond films characterized for a purity top worldwide level. The deposition is made on a silicon substrate, through a plasma obtained by applying microwave power to a hydrocarbon gas mixture injected in a tubular chamber. The usual technique of scratching is used to promote the nucleation of the diamond.

2.1 DIAMOND AS ALTERNATIVE MATERIAL TO SILICON

We have discussed the advantages and the possible and always more feasible microsystem applications. Is this enormous and recent development that has put in evidence the present technologies limits based in the use of silicon. In some applications, in fact, the resistance to high temperatures, high radiation flows and to chemical agents constitute the key decisive element to the use of a microsystem. It's now clear that the use of silicon as base material imposes limits to the application of a microsystem. It's known that silicon, still having remarkable electrical and mechanical properties, as well as good nuclear properties, present problems in harsh environments of diverse nature, which limit the use and therefore they prevent the fact to introduce microsystems there where they would be extremely useful. It's necessary then to study new materials, for microsystems, that they can unite the advantages of silicon the possibility of operating in hostile environments and that they are easily treatable with the purpose of making the elaboration necessary to obtain a microsystem.

Between "advanced" materials to be taken in consideration, *diamond* is, without any doubt, the most promising, with high potential applications, in particular in the field of radiation monitors and sensors. In fact, thanks to the high energy band gap (5,5 eV) between valence band and conduction band (apt to operate at high temperatures and in presence of light) and thanks to others remarkable physical properties, such as the high fusion point (4100 °C), low chemical reactivity and high mechanical robustness (Brinell hardness = 9000 kg/mm^2), diamond seems to be a natural candidate for electronics apt to operate in harsh environments. Others remarkable electronic properties are high carriers mobility (1800 and 1200 cm^2/Vs for electrons and holes respectively) and high breakdown field (10^7 V/m: 30 times greater than GaAs), this implies the possibility of operate at very high speed.

2.2 DIAMOND PROPERTIES

The diamond is constituted of carbon atoms in a tetrahedral lattice and is classified in crystallography as face cubic centered (fcc), the same as silicon. In particular, to any lattice point, a primitive base of two carbon atoms arranged in the (0,0,0) and (1/4,1/4,1/4) position is associated. The carbon atoms are hybridized sp3, anyone of them form four covalent bonds with the four nearest-neighbor, as illustrated in Fig. 2.1.

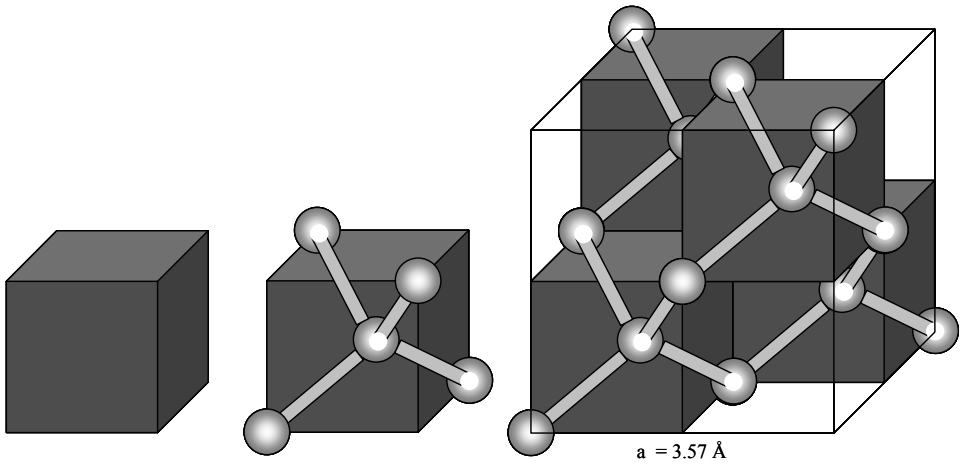

Fig. 2.1 Crystalline structure of diamond obtained by repetition of blocks tetrahedrally connected. The first neighbor define four faces of a cube, the cubs are grouped to make a cubic structure. In particular, it is reported the reticular constant a = 3.57 Å.

The nearest-neighbor distance is 1.54 Å, which is almost half of that of silicon. Because of that, diamond presents a remarkable lightness but a very compact structure, which confers a very interesting series of mechanical, thermal and chemical properties for a large number of applications.

Natural diamond is monochrystalline and depending of the nitrogen content and the form that it is placed in the crystal (substitutional, aggregate, etc.) it is classified according to the following scheme: type IA, IIA, IB and IIB. Type IA is the most abundant in nature and contents approximately 0.1% of nitrogen in the form of small aggregates; type IB contents nitrogen as interstitial impurity and almost all artificial diamond grown at high

pressure and high temperatures are of this type. Types IIA and IIB are very rare in nature and are characterized by extremely low nitrogen concentrations. In particular, IIA diamond presents optical and thermal qualities superior to other types, while type IIB presents optimal properties as semiconductor and it's of blue color. The main atomic, crystallographic, thermal and electrical properties of diamond are listed in Table 2.1, where are compared with that of silicon and germanium.

Table 2.1 Fundamental properties for diamond, silicon and germanium at 300 K.

Property	Diamond	Silicon	Germanium
Atomic Number Z	6	14	32
Mass Number A	12.01	28.09	72.60
Density (g cm^{-3})	3.52	2.33	5.33
Number of atoms (x10^{22} cm^{-3})	17.7	4.96	4.41
Crystalline structure	diamante	diamante	diamante
Reticular constant (Å)	3.57	5.43	5.66
Nearest-neighbor distance (Å)	1.54	2.35	2.45
Cohesion energy U (eV/atom)	7.37	4.63	3.85
Compressibility (x10^{11} m^2 N^{-1})	0.226	1.012	1.29
Work function ϕ (eV)	4.81	4.58	4.52
Fusion point Tm (°C)	~ 4100 *	1420	936
Thermal conductivity σ_T (W cm^{-1} K^{-1})	20	1.27	0.653
Diff. coefficient for electrons De (cm^2 s^{-1})	47	38	90
Diff. coefficient for holes Dh (cm^2 s^{-1})	31	13	45
Dielectric constant ε	5.70	11.9	16
E_{gap} (eV)	5.5	1.12	0.665
Pair energy electron-hole E_{pair} (eV)	13	3.6	3.0
Intrinsic carrier density n_i (cm^{-3})	< 103	1.5 x 1010	2.4 x 1013
Resistivity ρ_e (Ω cm)	> 1013	2.3 x105	47
Electron mobility μ_e (cm^2 V^{-1} s^{-1})	1800	1350	3900
Hole mobility μ_h (cm^2 V^{-1} s^{-1})	1200	480	1900
Breakdown voltage (V cm^{-1})	107	3 x 103	~103
Young modulus (GPa)	1134	131	103
Fusion temperature (°C)	3350	1410	937

* Carbon graphitization it's produced at 700 °C in presence of Oxygen.

2.2.1 Resistance to harsh environments

A fundamental aspect of diamond is his resistance to harsh environments. For example, in relation to chemical agents, it is inert to any chemical attack until the temperature of 900 °C, while for higher temperatures until the fusion temperature (3350 °C

at atmospheric pressure [19]) reacts in practice only with oxygen. The high fusion point represents another interesting aspect of diamond, allowing the engagement at high temperature environments. Diamond also shows a remarkable resistance to radiation of various types [20]; in particular, dose limits are always higher than then of silicon and it makes diamond attractive to operate in high intensity radiation fields.

2.2.2 Mechanical properties

Diamond is often used as abrasive in mechanical work due to his exceptional hardness. In fact, monochrystalline diamond is the harder material in nature, supporting pressures until 9000 Kg/mm^2. Moreover, diamond has the higher atomic density ($1.77x10^{23}$ cm^{-3}) at atmospheric pressure and a mass density of 3.52 gcm^{-3}. Another important characteristic of diamond is that it has the higher known Young's modulus (1134 GPa) that results practically independent from both, direction in which is measured [21] and temperature until 800 °C approximately [22].

2.2.3 Electronic properties

A direct consequence of the high compact lattice structure of diamond is the wide energetic separation (*gap*) between valence band and conduction band, which is near 5.5 eV. This gap is highly greater than that of silicon and allows considering pure diamond as insulator when it's maintained at room temperature [19]. In particular, this high difference in energy between valence band and conduction band allows to operate diamond microsystems in temperatures highly greater than room temperature, till 600 °C, without notice about a signal saturation linked to the pass of a high number of electrons in conduction band. However, in the case of silicon, temperatures little higher than room temperature are enough to produce a saturated signal, then destroying the semiconductor

properties of the material and avoiding the device operation. The high value of the energy gap E_{gap} confers to the diamond a high resistivity ($\rho \sim 10^{15}$ Ωcm, in light absence), that allows to produce intrinsic diamond devices, different to silicon, for which is necessary to make junctions to obtain the same result. Also the high breakdown field, 10^7 V/cm approximately, depends on the value of the E_{gap}. In particular, the union between these properties with thermal characteristics, which follow, allows obtaining microsystems that are able to absorb high power respects to their own dimensions. This is a remarkable advantage, because high power dissipation requires non-trivial volumes. It is known that in presence of an opportune doping element diamond shows piezoresistive properties [23], useful to project a microsystem apt for electromechanical measurements (pressure, acceleration), also operating at high temperatures [24].

2.2.4 Thermal properties

Thermal conductivity of diamond is about 20 W/cm K and results 5 times greater than that of cupper and comparable with that of materials as lithium fluoride (LiF) and aluminum oxide (Al_2O_3). This good thermal conductivity is very important for the mechanical elaboration, where is necessary to rapidly transfer the heat produced by the elaboration. We observe that high thermal conductivity seems to contrast with the fact that at room temperature diamond is practically an insulator. The point is that the particular diamond structure, extremely compact, joined to the lightness of carbon atoms from which it's formed, made extremely easy phonon transport in diamond, for which, in effect, heat transport depends on the phonons instead of electrons [25]. In particular, the possibility of heat dissipation while being an insulator made possible, at least in perspective, the elaboration of mixed systems diamond/silicon (diamond as we will see grows on diamond)

in which on the silicon are made the electronics or the microsystems, while diamond act as heat dissipator.

2.2.5 Optical properties

Also from the point of view of optical properties diamond shows very interesting characteristics. It is practically transparent to radiation, from far infrared to the ultraviolet, corresponding to the gap at 225 nm (5.5 eV). In particular, it's observed weak transitions at two or three phonons in the 1332 – 2664 cm^{-1} and 2665 – 3994 cm^{-1} intervals, which represent the only zones of intrinsic absorption. Other types of absorptions must be imputed to the impurities [26]. This optimal transparency characteristic, together with that of resistance, make diamond an ideal material for the production of optical windows for power lasers or connect optically harsh environments [22].

2.3 DIAMOND GROWTH

Diamond properties just reported allow to understand how could be important the application of this material in many fields. In the other hand, at it's known, natural diamond besides being little abundant in nature could be also very expensive (if we think in IIB type) and it's presented as monochrystalline type which geometries and dimensions are difficult to practical use. So, it was necessary to study production techniques of artificial diamond in order to obtain this material easy to use for microsystems production and with the possibility of modifying some specific properties only varying in the right way the growth process parameters. Then, it is presented the most common production techniques for diamond, both, monochrystalline, that is based in the engagement of high pressures and high temperatures, and polycrystalline, that use low pressure methods. We

note that in the first case the growth occurs in the region of the phase diagram of carbon, illustrated in Fig 2.2, for which diamond is in the stable state, while in the second case diamond grows, at smaller pressures, in the region where graphite is in the stable state and diamond in the metastable state [27].

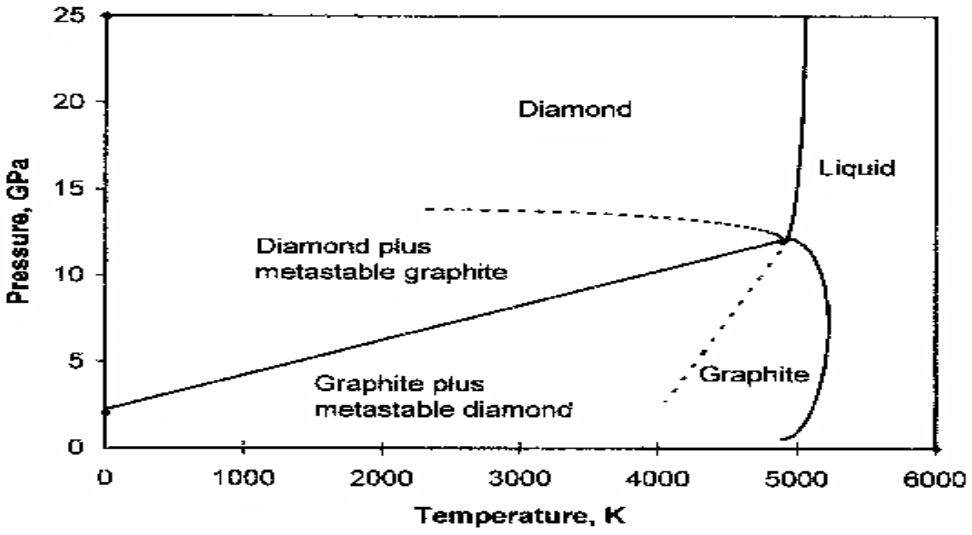

Fig. 2.2 Phase diagram of carbon. Regions of metastable diamond and graphite are limited by dot lines, that are extensions of the lines that separate diamond and graphite stable from liquid phase.

2.4 HIGH PRESSURE AND HIGH TEMPERATURE (HPHT) GROWTH METHOD

This method is similar to the natural formation of diamond monocrystals; it means a high pressure (60 GPa approximately) and high temperature (till 1600 °C) environment for diamond growing from carbon. In the laboratory it is used the knowledge of the carbon phase diagram (Fig. 2.2) and graphite as base material. Nowadays with the HPHT [28] technique the biggest diamond crystals are produced (till some cubic millimeters), but are characterized for a high impurity level, irreducible in this growth conditions. This doesn't limit the use in the microsystems field, for which mechanical elaboration represents the

main application field for this type of artificial diamond, but with production costs non-trivial, for which sometimes the use of natural diamond is more convenient.

2.5 LOW PRESSURE GROWTH METHODS

The introduction of low pressure methods allowed enormous progress in artificial diamond synthesis [29-31], for which the study and use of this methods is at the present very diffused and we can say that today artificial diamond growth with these methods presents many properties similar to those of natural diamond. In the low pressure methods diamond is deposited with the *Chemical Vapor Deposition (CVD)* technique. In particular, carbon is supplied as an opportune chemical composed (for ex: CH_4) in gas or vapor phase. Carbon is then chosen supplying energy to the gas in order to divide the molecule in which the gas is fixed. This could be obtain by heating or with radio frequency, and the use of a technique instead another, as well as the chose of the gas mix in gas or vapor phase, differentiates between the different available techniques for CVD diamond growth.

2.5.1 Hot filament method

In this method (*Hot Filament Chemical Vapor Deposition or HFCVD*), the general scheme is reported in Fig. 2.3 [32], the necessary energy for diamond deposition is provided by a hot metal filament (generally made of tungsten) placed some millimeters from substrate (made of silicon or molybdenum) where will take place diamond deposition [33]. In particular, the filament is electrically heated till 2000 °C approximately, while the deposition chamber is maintained at 700 – 1000 °C. The inlet gas mix is composed by methane (1% in volume) and hydrogen, diluted in nitrogen. The chamber pressure is maintained in the 1 – 10 KPa interval.

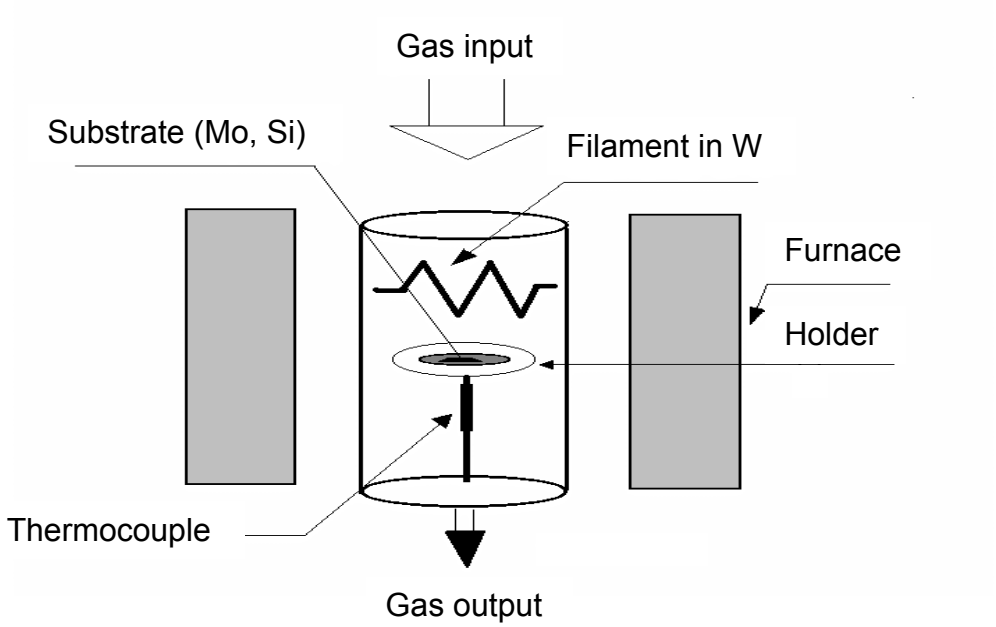

Fig. 2.3 General scheme of a *hot filament deposition* apparatus.

The HFCVD method is in principle very simple and economic and is surely the most diffuse. The most interesting aspect of this technique is represented by the flexibility in form and dimensions of the films that could be deposited. Moreover, the deposition rate is similar to others CVD techniques, being in the 0.1 – 1 μm/h interval. However, between the problems related with this technique must be noted the high impurity concentration and a low stability of the deposition process.

2.5.2 Combustion flame deposition

The *Combustion Flame Deposition (CFD)* owes his name to the fact that the necessary excitation energy for diamond growth is supplied by a flame generated from the combustion of a hydrocarbon gas (typically acetylene) with oxygen [34]. In particular, the growth substrate, mounted on an appropriate sample holder, is exposed directly to the flame and water cooled, as illustrated in Fig. 2.4.

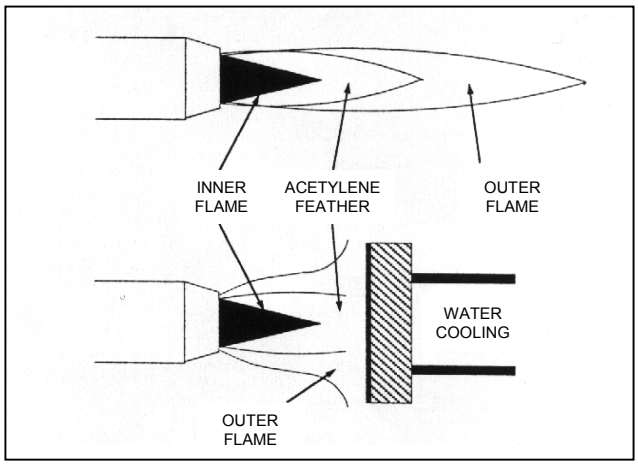

Fig 2.4 General scheme of a *combustion flame deposition* apparatus.

This method is very simple and presents high growth rates (till 50 μm/h); however, the quality of the obtained diamond, specially for optical, electronic and purity characteristics, cannot be compared with that obtained by hot filament nor that obtained by plasma enhanced deposition, which follows. Nevertheless, diamond obtained by CFD method maintains good thermal and mechanical properties that make it appropriate for instruments coating for mechanical work.

2.5.3 Plasma jet deposition

The *Plasma Jet Deposition (PJD)* is a technique that use a plasma to supply the necessary energy to the diamond growth [35]. The substrate is placed at the exit of a plasma source, in a vacuum environment (10 KPa approximately). The typical used gases are hydrocarbons with the addition of hydrogen. In particular, the use of oxygen could improve the quality of the produced films. The general scheme of some PJD deposition systems for diamond is illustrated in Fig. 2.5.

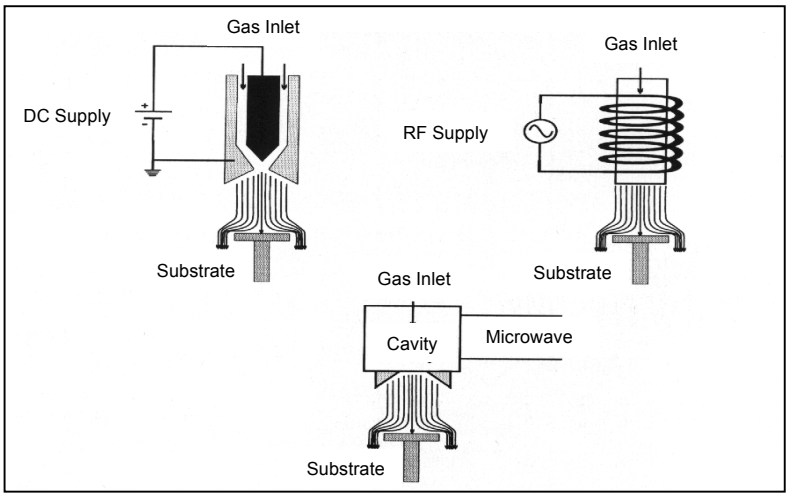

Fig 2.5 General scheme of a *plasma jet deposition* apparatus.

The PJD presents a high growth rate (till 100 μm/h) and the quality of the films produced are superior to those obtained by combustion flame deposition, above all for optical properties. Problems become when it is intended to obtain homogeneous areas superior to 1 cm^2.

2.5.4 Plasma enhanced deposition

Microwave Plasma Enhanced Chemical Vapor Deposition (MPECVD) [35,36] is characterized by the high purity of produced films and then particularly interesting for microsystems production, even though, for problems related to the power density of the plasma, it's not appropriated for large areas production (> 100 cm^2) and could not be applied for non-planar areas production. The main idea is to use a plasma to supply the necessary energy for the activation of the chemical deposition of the vapor phase and in general microwaves at 915 MHz or 2.45 GHz are used. A typical reactor for plasma enhanced CVD diamond growth is illustrated in Fig. 2.6 and is referred to the apparatus that is used at the Mechanical Engineering Department of the University of Rome "Tor Vergata" laboratories [37,38].

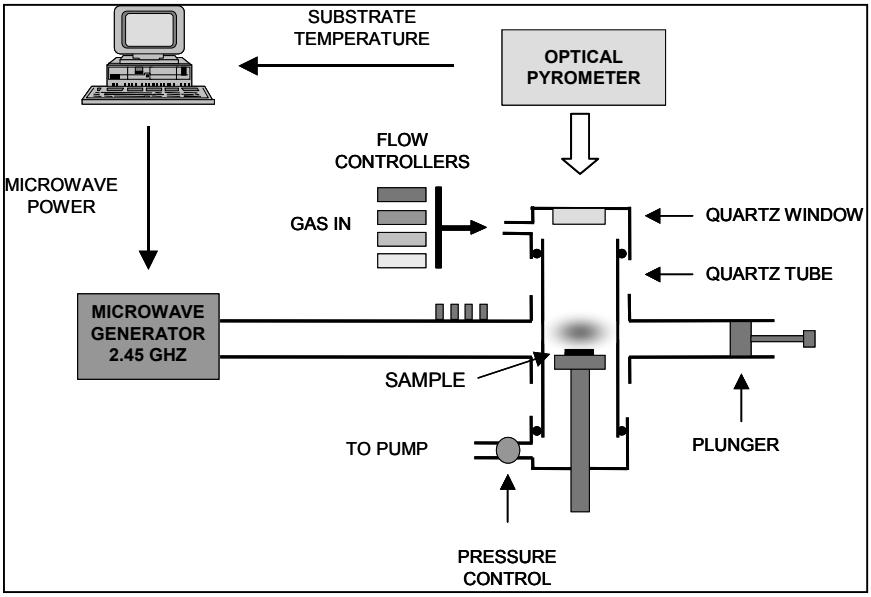

Fig. 2.6 General scheme of the apparatus used in the present work for CVD diamond films deposition.

It is constituted of a vacuum chamber, with gas flow controllers, inside which is a sample holder made of steel, water cooled, on which is placed the silicon substrate where diamond will grow. Microwaves, generated by a magnetron at 2.45 GHz, are propagated within the chamber (which acts as a resonant cavity) through a waveguide. Microwaves yield its energy to the plasma electrons, which at his time yield the energy to the gas through collisions and then heating it [39]. The chemical reactions, which follow the heating, move towards the formation, between others composed, of carbon, which is then deposited on the silicon substrate, giving place to a diamond film growth. It's worth underline that diamond growth is obtained only if on the substrate surface are present nucleation centers (obtained by a pre-treatment of the substrate) and growth parameters (gas composition, pressure, plasma temperature, microwave power density, etc) are chosen in the appropriate way. In particular, the grow rate of diamond with this method vary from 0.2 μm/h to 10 μm/h, depending on growth parameters and chamber geometry.

2.6 CVD DIAMOND FILMS PRODUCTION

We've seen a typical scheme of a PECVD diamond film reactor (Fig. 2.6) and in particular we referred the diamond film deposition apparatus used for the present work. In this type of reactor, microwaves give energy to the electrons of the plasma, which, at his time, give energy to the gas through molecular collisions, heating it. The chemical reactions, which follow this heating, allow the formation of carbon that is deposited on the silicon substrate. The various monocrystals derived from the nucleation centers grow till make a continuous film. In particular, when growth goes on, some crystals are "submerged" from others called "dominants" and grains are always bigger. This gives, as a result, the typical columnar structure for diamond films, as it is clearly shown if we look a polycrystalline diamond film in section through a scanning electronic microscope (SEM) (Fig. 2.7).

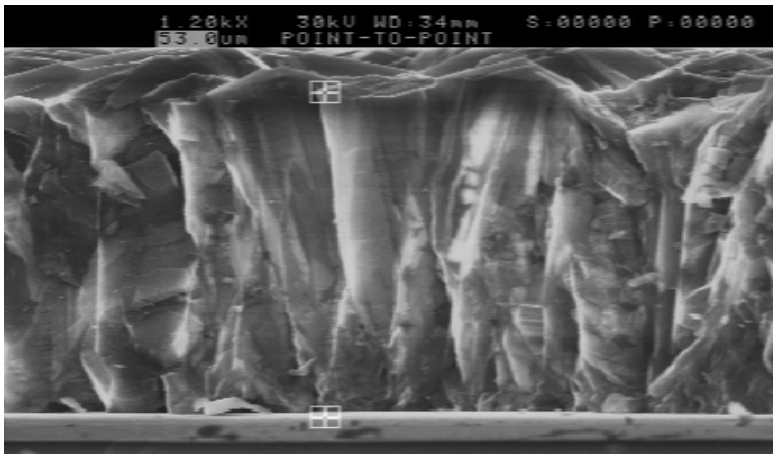

Fig. 2.7 Cross section of a polycrystalline diamond film seen at the Scanning Electron Microscope (SEM).

2.6.1 CVD diamond growth and nucleation

It is appropriate to notice that diamond growth occurs only if the substrate surface is the opportune one, it means if we're in presence of nucleation centers. With this purpose, the silicon substrate is pre-treated in order to favor diamond nucleation. In

general, this pre-treatment is made through a technique called "scratching", which consists in submerging the silicon substrate in an ultrasonic apparatus in which is contained an abrasive solution (typically micrometric diamond dust in acetone). The collision of abrasive particles produce on the substrate surface micro-scratches, which represent the nucleation centers. Alternatively it could be used the *"biasing"* technique, it consists in produce the nucleation centers directly on the silicon substrate placed in the vacuum chamber. In practice, in plasma presence, a potential difference of hundred of volts is applied in order to generate a high flux of plasma ions to the substrate. The collision of these ions on the silicon surface produces micro-scratches that remarkably increase the nucleation.

Once created the nucleation centers, the diamond growth could be done. It is worth notice that in low pressure methods the growth is obtained in the steady state of graphite in the phase diagram of carbon, while diamond is unsteady. Therefore, in order to allow diamond growth it's necessary to create a formation barrier to the graphite and this is the role of the hydrogen in the growth process. In fact, most accepted theories [40] assume that is a simultaneous deposition of hybridized carbon sp^3 (diamante) and sp^2 (graphite). The formation of diamond is facilitated by the presence of hydrogen because it's placed on the film surface reacting with the free bond of the carbon from the hybridization sp^2 [41]; by this way it's formed on the diamond surface an uniform saturated hydrocarbon layer that inhibits the single atom species to be deposited on the surface. So, hydrogen presence must suppress nucleation and growth of unsaturated graphitic structures. In fact, it's noted that the presence of molecular hydrogen diminishes dramatically spontaneous nucleation and graphite deposition. Nevertheless, only molecular hydrogen cannot full suppress graphite growth: graphitic carbon can; in fact, nucleate on the diamond surface and ulterior

suppress the same diamond growth. Then, it is necessary to remove graphitic deposits using atomic hydrogen.

2.6.2 C/H/O Diagram

Theory and experience show that the choose of gas mix and his purity play a fundamental role in the produced diamond quality and in its growth rate. As it was told, the chemical species to be used are essentially carbon and hydrogen; the presence of oxygen could bring the increment of the growth rate. In particular, the concentration of the gases to be used for diamond growth could be visualized through a ternary diagram proposed by Bachmann [42] and shown in Fig. 2.8.

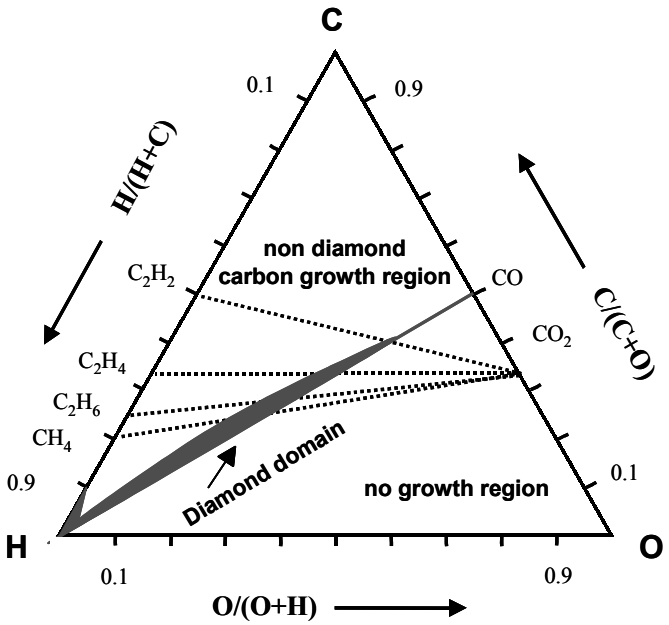

Fig. 2.8 Ternary diagram of gas concentration present in the growth chamber (Bachmann's diagram).

The diagram is a triangle in which any side reports the relative concentration of the three atomic species C, H and O generally present in the gas mix used for diamond growth. In particular, three regions are distinguished: a region of no growth, a graphite growth region but non-diamond and a diamond growth region. As is evident, the last one is closed

between the first two, that are preponderates. The diagram clearly shows how diamond could be obtain even in absence of oxygen. In this case, the most used gas mix is composed of little quantities of methane in hydrogen. However, it's possible to obtain diamond also in presence of oxygen, but in this case growth is verified only if carbon concentration is lightly superior to that of oxygen, that's because there is formation of CO and diamond is deposited only if sufficient carbon atoms remain. At the end, diagram reports the concentration lines of C, H and O for gas mix most common used ($CO_2 – CH_4$, $CO_2 – C_2H_6$, $CO_2 – C_2H_4$, $CO_2 – C_2H_2$).

It's worth underline that a fundamental aspect to obtain good quality diamond is represented by the purity of the used gases. The presence of impurities in the gas mix allow their deposition and then to the formation of defects from various type and nature in the diamond crystal. To this purpose we notice that because CVD technique works at lower temperatures, diffusion and then concentration of polluting agents inside the crystal are lower than other production techniques of diamond.

We observed, as it was told before, diamond growth happens with the typical columnar structure and an interesting aspect of this type of growth is the growth rate dependence of the different crystallographic faces from growth parameters. In particular, it's possible to vary the relative growth rate of various faces and then, controlling and acting on growth parameters (for ex: temperature or methane concentration [22]), it's possible to favor some crystallographic orientations instead others and selecting, by this way, the characteristics of the desired film [43].

2.6.3 Optimization of growth parameters

The development and sharpening of the microwaves CVD technique at the Mechanical Engineering Department of the University of Rome "Tor Vergata" laboratories

and the characterization of obtained diamond films was discussed in three precedents PhD thesis [38,44]. In particular, growth parameters optimization studied in those works allowed to produce CVD diamond of excellent quality [45].

The present thesis is a natural continuation from precedents, emphasizing the reliability of the used growth technique, sample reproducibility and diamond doping.

In particular, during the PhD period, a new growth chamber was mounted, with the scope in deepening the knowledge acquired by the group in the last few years. The mounted apparatus is similar to that of Fig. 2.6. It's composed by a tubular microwave CVD reactor, in which the growth chamber is constituted by a 60 mm quartz tube maintained in vacuum, microwaves are generated by a commercial magnetron of 2.45 GHz and a power of 2 KW. The silicon substrate (pre-treated with the *scratching* technique) is placed on a sample holder made of steel, in direct contact with the plasma, cooled by water. The substrate temperature (fixed in the 650 – 850 °C range) is continually measure through an optical infrared pyrometer and automatically controlled by a system *ad-hoc*, via software, which regulates, in retroactive way, the power of the magnetron in order to maintain constant the substrate temperature.

The gas flow is controlled by four flowmeters. It is worth notice that for the precedent growth chamber was used, through the time, different gas mix for purity and composition: $CH_4 – H_2$, $CO_2 – CH_4$ and $CO_2 – C_2H_6$. In particular, a systematic study for the quality of the produced film varying the methane concentration [44] had indicated as the optimal mix that of $CH_4 – H_2$ at 1% of methane, because of that it was chosen as the gas mix for diamond growth in the new chamber.

It is important to underline that the new chamber has obtained immediately results of remarkable interest, allowing the realization of high quality diamond films, which made more promising future works in order to optimize growth parameters. Another important

aspect of the work developed in the PhD period is the realization of p-doped diamond with the scope to realize doped diamond samples that allow the possibility of doing sensor prototypes and to study the behavior of diamond as a piezoresistor to be study at different temperatures, moreover, the realization of doped diamond started another important prototype development, which is the realization of a diamond thermocouple; all these projects are immersed in the R&D and collaboration strategies of the Mechanical Engineering Department of the University of Rome "Tor Vergata" diamond laboratory.

2.7 PATTERNING AND APPLICATIONS OF CVD DIAMOND

Coming back to microsystems, we observe that polycrystalline diamond could be used in micro patterning, but based on different principles of that of microlithography. In fact, the main difficulty in diamond *patterning* derives from the same characteristic that makes diamond an apt material to operate in harsh environments, it means, resistance to physical and chemical actions, which are often engaged in conventional lithography. In particular, diamond could be attack with plasma in presence of oxygen or we could take advantage that diamond grows on silicon but not on silicon oxide, for which it's possible to induce a "*selective growth*", for example through an opportune mask that allows to oxidize selectively some regions instead others on the silicon substrate. Another way consists in favor diamond nucleation on a pattern obtained by scratching on the substrate surface through abrasive solutions.

Regarding diamond applications, in literature is reported, for example, the realization of temperature sensors [22]. In particular, termistors have been produced apt to operate in a wide interval of temperature and, the most important, in high temperatures environment [46]. Moreover, because of CVD diamond presents piezoresistive

characteristics [47], it was used this property to produce pressure sensors [48]. At the end, it was reported various applications of CVD diamond in electronics [22]; in particular, diodes and transistors were done [49,50].

We conclude this chapter underlining that, in order to take totally advantage of possible applications of diamond, it's necessary first of all to have good quality diamond, for which is fundamental the study of the physical properties of the produced diamond, with the scope of better understand its characteristics and to optimize growth parameters.
In fact, polycrystalline nature of CVD diamond and its relative high structural defects represent, at the moment, a limit to possible applications, for example, that of radiation detector.

Chapter 3

Growth and characterization of boron – doped CVD diamond films

Summary

An important aspect related to the realization of diamond-based devices is constituted by the possibility of making doped films. In fact, there are numerous applications that require the use of films of this type [51-53]. Although p-type diamond films are reported in literature, at the present no group of investigation has yet succeed in produce n-type diamond films with appropriate properties to be used in microsystem field. In spite of, recently interesting developments have been published in n-type diamond production, [54] it's still difficult to make diamond p-n junctions. Nevertheless, most part of diamond applications in microsystems field need only one doping type. An important characteristic of opportunely doped diamond is the piezoresistive property. It's well known that doped diamond, with boron, presents interesting piezoresistive properties; this property is extremely important because, due to the large gap of diamond, it's possible to produce devices sensible to mechanical stress (i.e.: pressure, force, acceleration, etc) that can operate at high temperature. The possibility of making high pressure measures at high temperature (beyond 400 °C) is highly required by industry for process control. Because it doesn't exist sensors apt to operate at high temperature, these types of measurements, at the present, are effectuated transporting mechanically the signal to be measured in low temperature zones. This procedure, besides complicate the measure system, often introduces an inevitable worsening in measure sensitivity. With the scope of realizing a piezoresistive strain gauge demonstrator, it was made an apparatus for the deposition "*in situ*" of p-type doped diamond films. In order to evaluate growth samples, they've been characterized through measures of resistivity in function of temperature. An other important parameter that is the Temperature Coefficient of Resistance (TCR) was calculated in order to evaluate the sensibility of diamond to little change in resistance, this parameter will tell us the necessary accuracy in temperature measurements of piezoresistive effect with which we will have to deal in order to put in manifest the relative change in resistance due to piezoresistive effect that must not be hidden by relative changes in temperature due to TCR variations; in order to do that, little tolerances in temperature variations must be admitted to put in manifest piezoresistive effect.

3.1 USED EQUIPMENT IN CVD DIAMOND P-TYPE DOPING

P-type doped diamond deposition was done introducing boron in the growth chamber during deposition. It's well known that boron is a strong contaminant of the growth chamber, in fact, after a growth with the addition of boron it's very difficult to totally clean the chamber. Because of that, the successive films grown present impurities of this material; it's then fundamental, to separate the chamber use for doping growth and for intrinsic one. It's worth to note that boron doped diamond samples grow on intrinsic diamond substrates, which at this time grow on commercial p-type silicon substrates (100) orientated and with a resistivity of 20 Ωcm and 525 μm thickness.

MPECVD (*Microwave Plasma Enhanced Chemical Vapor Deposition*) growth apparatus (described in chapter 2.5.4) was substantially modified putting, throughout the waveguide, another growth chamber in series with the previous one. In Fig. 3.1 is shown a scheme of the growth chamber. The bigger chamber, in red, was added in order to obtain two separate chambers. In particular, the "small" one is used for doped diamond growth and the "big" one is used for intrinsic diamond growth.

In order to introduce boron into the chamber a methanol (CH_3OH) and boron dioxide (B_2O_3) solution is used. The choice of this mix is essentially due to the fact that, in addition to the boron, in the growth chamber are only introduced carbon, hydrogen and oxygen; as we saw before, they don't introduce impurities or defects at the internal of the diamond. Another possibility for boron doping is to use diborane (B_2H_6) in the growth chamber. The problem of using this gas is that it is lethal even at very low concentrations and the use of this gas requires extremely expensive and complex security measures.

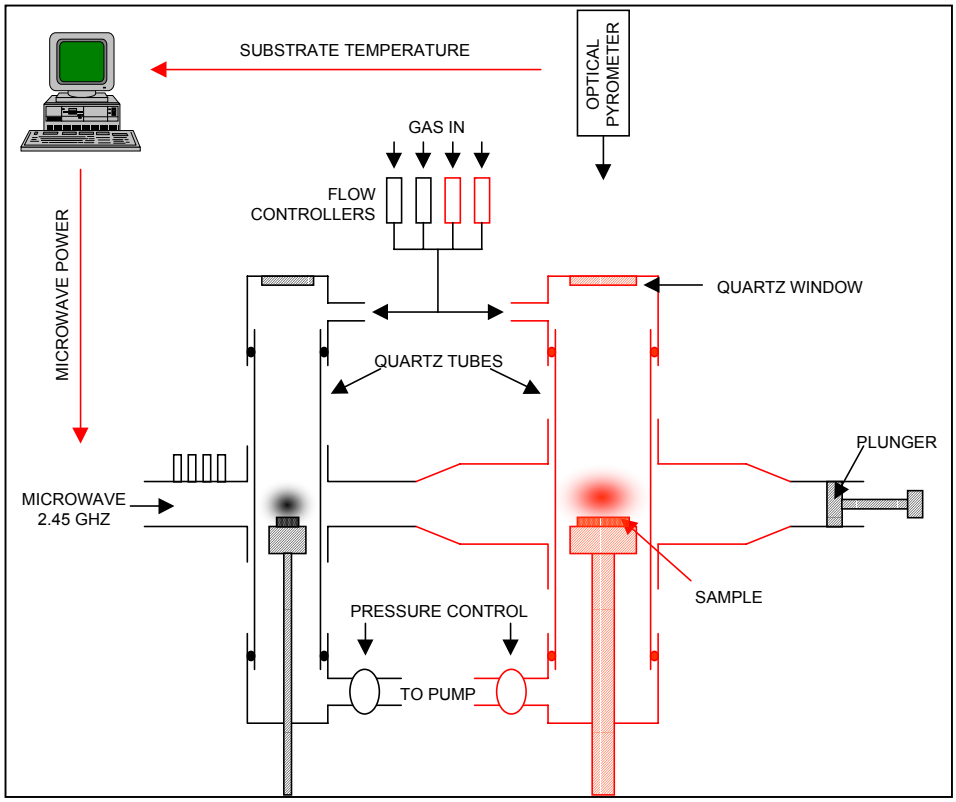

Fig. 3.1 General scheme of the growth chamber used at the Mechanical Engineering Department of the University of Rome "Tor Vergata" laboratories, in particular, the black one is used to grow intrinsic diamond films and that in red to grow boron-doped diamond films.

Fig. 3.2 Photograph of growth chamber used at the Mechanical Engineering Department of the University of Rome "Tor Vergata" laboratories.

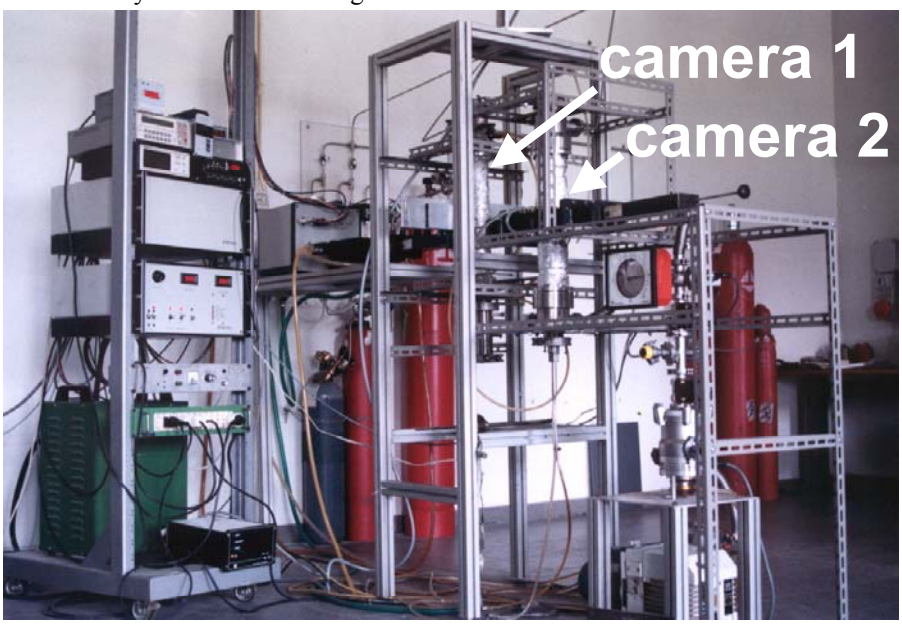

The methanol – boron dioxide solution is introduced in the growth chamber in vapor form through a flow-meter, which is illustrated in Fig. 3.3. In order to avoid methanol condensation in the flow-meter, this one is heated at approximately 40 °C. This system allows controlling the entry of methanol and boron vapors in the growth chamber with a resolution near 0.01 sccm.

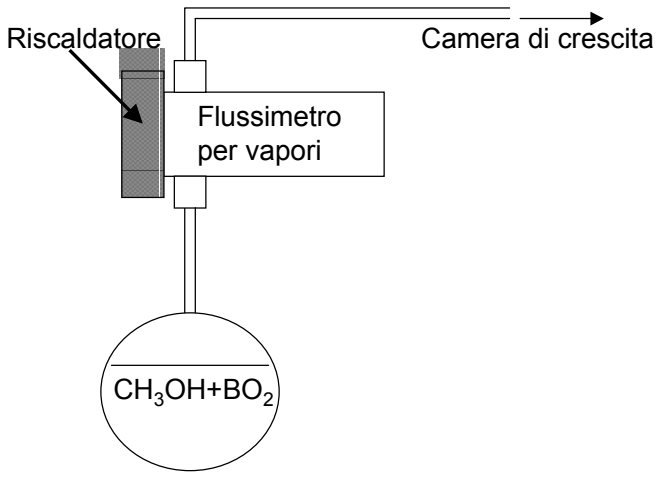

Fig. 3.3 Scheme of boron doping system, an accurate control of the gas is done in order to feed the growth chamber.

3.2 CONDUCTION MECHANISMS IN P-DOPED CVD DIAMOND FILMS

Infrared absorption measurements, cathodoluminiscence measurements and photoconductivity measurements have shown that acceptor centers in synthetic semiconducting diamond is the same as that in natural semiconducting diamond. Physical diamond theory shows that the same acceptor center was responsible for the electrical properties of natural and synthetic semiconducting diamond, and the behavior of heavily doped diamonds was interpreted in terms of impurity conduction [55]. The D.C. conductivity of a sample can be expressed as a sum of three components [56]:

$$\sigma = \sigma_1 \cdot e^{\frac{-E_1}{K_B T}} + \sigma_2 \cdot e^{\frac{-E_2}{K_B T}} + \sigma_3 \cdot e^{\frac{-E_3}{K_B T}} \qquad (3.1)$$

The activation energy E_1 is the normal acceptor ionization energy and is observed in all samples where the acceptor concentration is not too high. The activation energy E_2 is associated with conduction in an impurity band; for low acceptor concentrations $E_2 \sim E_1$, but as the acceptor concentration is increased, E_2 become smaller than E_1 and finally at the acceptor concentration for which the metal-insulator transition occurs $E_2 \rightarrow 0$.

The activation energy E_3 is most prominent for samples with a relatively low impurity concentration and is interpreted in terms of the energy associated with the transition of a positive hole from an occupied to an unoccupied acceptor site.

In equation (3.1) $\sigma_1 > \sigma_2 > \sigma_3$ and $E_1 > E_2 > E_3$, therefore at high temperatures the conductivity of all specimens is dominated by the first term. At lower temperatures the second and/or the third term, depending on the acceptor concentration, will govern the conductivity. If this is sufficiently high the conductivity will be temperature independent at low temperatures. The changeover from one conductivity mechanism to another is indicated by a change in the slope of the log ρ versus T^{-1} plot with a fairly sharp knee, as is illustrated in Fig. 3.4.

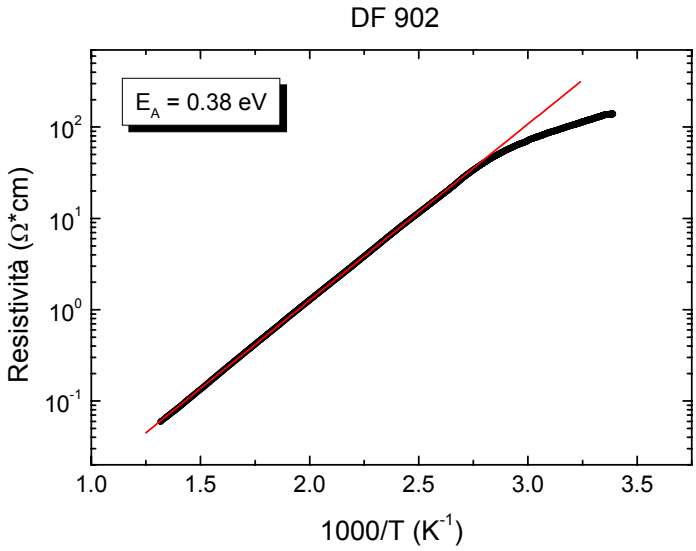

Fig. 3.4 Graphic of Resistivity as a function of 1000/T, the change in the slope of the curve show a change in conduction mechanism.

An interesting conduction mechanism to be explained is, at high doping levels, which that is known as "hopping conduction" in which an appreciable overlap effect between the orbits of adjacent impurities atoms occur. This overlap tends to produce an impurity band (a band of energy levels which permit conductivity) in which electrons move from an impurity site to a neighboring ionized impurity site [57].

3.3 CHARACTERIZATION OF P-DOPED DIAMOND FILMS

The presence of boron impurities inside diamond produces the presence of acceptor states in the band gap. By effect of thermal agitation this states could be occupied by electrons coming from the valence band; producing, then, a number of holes in valence band equal to the occupation of the mentioned states. This phenomenon is responsible of the conductivity of a doped film and, in particular, conductivity is proportional to the

number of holes present in valence band and then to the occupation number of the acceptor states.

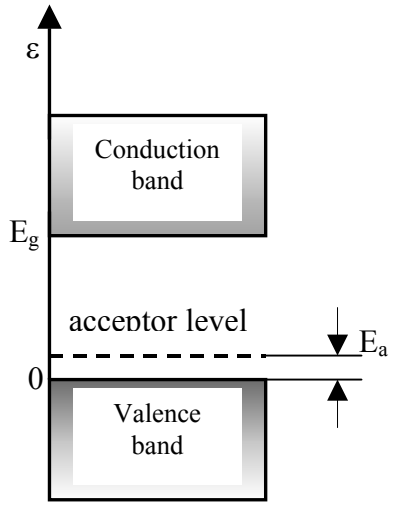

Fig. 3.5 Band scheme of a typical semiconductor showing Eg the energy gap and Ea the activation energy.

If E_a (activation energy) is the energy between the valence band and the energy level of the acceptor states, at it's shown in Fig. 3.5, the occupation number could be calculated through the Fermi distribution. In particular, it's known that the occupation number of the E_a state is proportional to the $exp(-E_a / k_BT)$ factor. In consequence, resistivity could be written as:

$$\rho = \rho_0 \cdot e^{\frac{E_a}{K_B T}} \qquad (3.2)$$

Where "K_B" is the Boltzmann constant and "T" the temperature; it's then possible to calculate the energy level produced by impurities measuring resistivity as a function of temperature. In particular, plotting log ρ as a function of the inverse of temperature it's obtained a slope of coefficient E_a / k_B. The measure of resistivity as a function of temperature is, then, an important characterization method, while because allows to

quantify the effective doping contribution inside the crystal either because allows the determination of the introduced acceptor energy level.

3.3.1 Characterization through R(T) measurements

In order to realize the measurements of resistance as a function of temperature, the following steps must be accomplished in the standard procedure. First of all, once a boron p-doped diamond sample is retired from the growth chamber, it must be subjected to a procedure known as "*thermal annealing*", which consists in putting into an oven at 500 °C for one hour the diamond sample in order to remove the superficial hydrogen which in fact constitute a conductive layer for diamond. After that, two silver paint contact are made on the diamond surface, in general this contact are made at a separation length of 2 mm each other, then, in order to stabilized the contacts, another "*thermal annealing*" process is done, this time is one hour at 400 °C. Once this processes are done the sample is put in a sample holder, then, contacted with Pt wires and connected to a multimeter in order to read the resistance by an appropriate acquisition system (GPIB cards). A computer program takes the measures coming from the multimeter that reads the resistance and from another multimeter connected to a thermocouple placed in the oven to read temperature. At this point, when the oven is on, the temperature increases till 470 °C, once arrived, the oven is switched off and the measure starts; the idea of making the measure with the temperature "descending" guarantees a higher homogeneity in the measure. Because the multimeter reads the resistance of the sample, resistivity can be calculated by the following equation:

$$\rho = R \cdot \frac{S}{l} \tag{3.3}$$

In which "S" is the transversal conductive section of diamond, and "l" is the distance between contacts, as is shown in Fig. 3.6. Because "l" is greater than contact dimensions and the film thickness Eq. 3.3 is an acceptable approximation of resistivity.

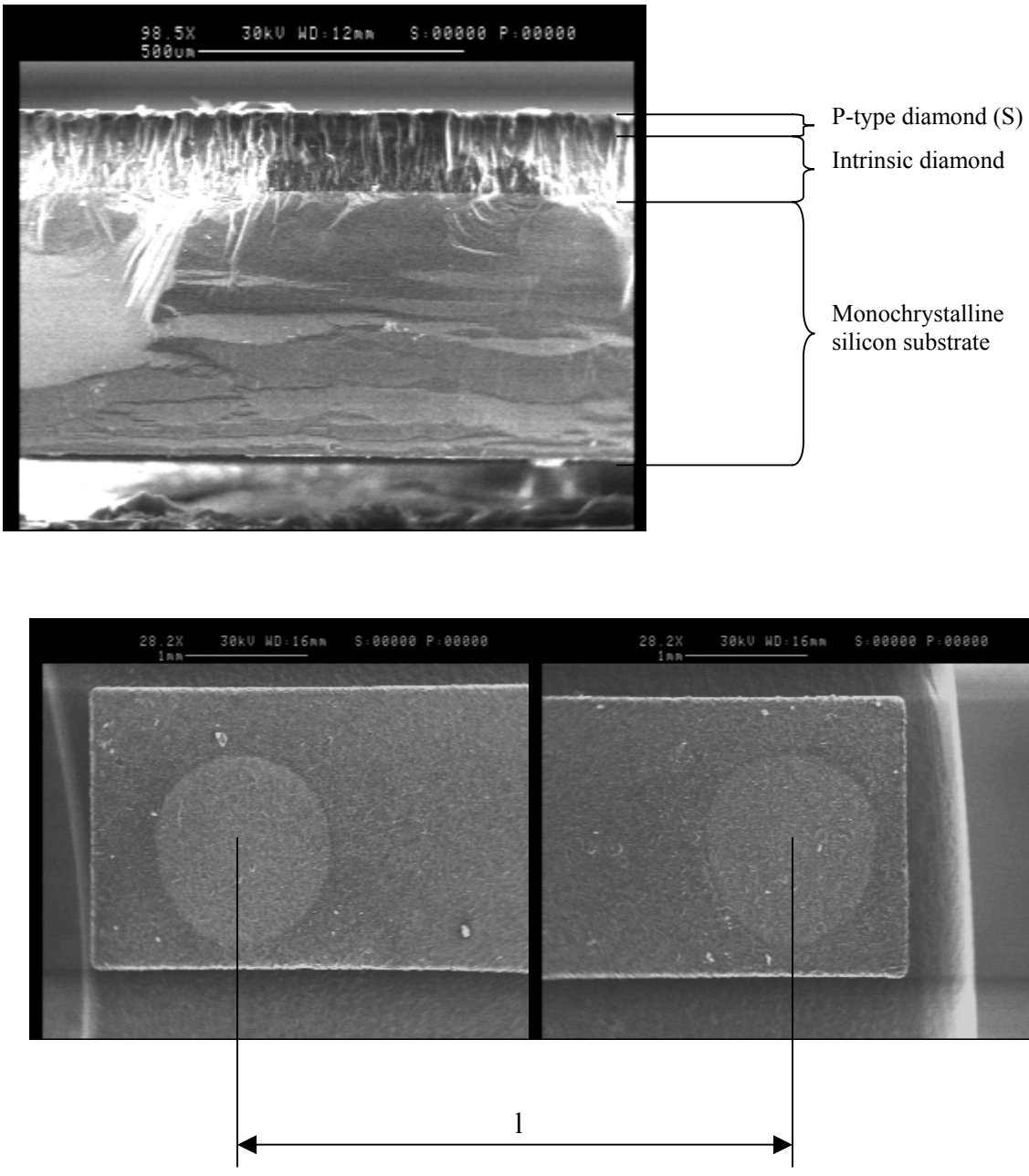

Fig. 3.6 The upper SEM photograph shows the cross section of a diamond sample, where it's shown the monochrystalline silicon substrate and the grown diamond, notice the columnar nature of diamond growth. The lower SEM photograph shows two broken pictures of the diamond sample, it is shown the circular gold contacts and the dimension "l" between them.

3.3.2 Temperature Coefficient of Resistance (TCR)

As a semiconductor diamond change its resistivity as a function of temperature, following this resistivity change an exponential law (see Eq. 3.2). We can define a magnitude that give us an idea of the sensitivity of diamond with temperature changes, this magnitude is the "so called" *Temperature Coefficient of Resistance (TCR)* and it's defined through the following equation:

$$TCR = \frac{1}{R} \cdot \frac{dR}{dT} \tag{3.4}$$

In Fig 3.7 it is shown the TCR for different boron-doped diamond samples; as we can see, it is strongly dependent on doping level, thus in resistivity, since it's clear that Eq. 3.4 uses R(T) measurements, defined in subchapter 3.3.1, to calculate it.

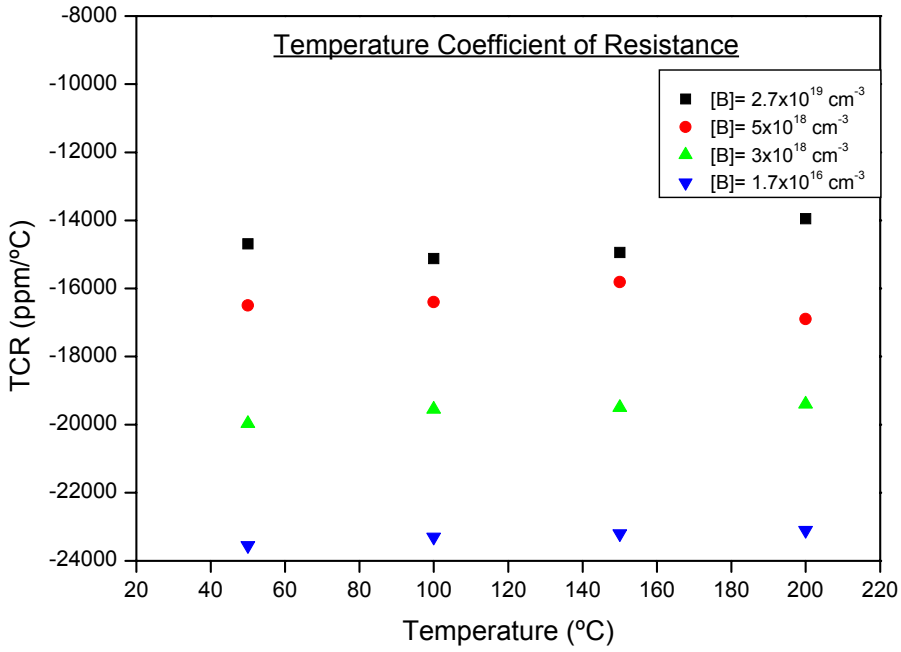

Fig. 3.7 Graphic of TCR as a function of temperature for different boron-doped diamond samples with different doping levels.

As we can see from this graphic there is a clear trend in increasing TCR with decreasing doping level for doping level lower than 10^{18} cm^{-3}. At it is evident the graphic in Fig. 3.7 is limited to 200 ºC, TCR for higher doping level samples reaches a value as lower as 1000 ppm/°C at 450 °C, increasing its value with decreasing doping level. That fact means that measurements of piezoresistive effect, as we will see in seventh chapter, must have an accurate control of temperature specially those samples with lower doping level; if not, we risk to measure changes in resistance due to little variations of temperature instead relative change in resistance due to piezoresistive effect, hiding by this way, the mentioned effect.

3.4 DOPING GROWTH CHAMBER DYNAMICS

In order to understand the characteristics of the growth chamber used for doping, was developed during the PhD period a systematic study of the doping dynamics of the chamber. In particular, two studies were made; the so called "*doped at once and growing*" which consists in growing a boron doped diamond sample and the successive grow of diamond samples without any presence of dopant gas mix. The second systematic study was the so called "*doped at once and growing in presence of methanol*", the scope of the systematic study of the last one is to understand the inhibitor effect observed in the boron-doped diamond samples because of methanol presence; for these one, experimental curves of resistance (resistivity) as a function of the temperature were made. Further, theoretically analysis was made in concordance with scientific published literature.

3.4.1 Doped at once and growing systematic study

In this part of the work, the main idea was to established how the growth chamber reacts to the successive growths in a previously contaminated (with boron) environment, for this reason, a diamond sample was grown with 0.2 sccm gas flow of boron oxide (50 mg) in methanol (CH_3OH); Fig. 3.8 shows the resistivity as a function of temperatures experimental curves.

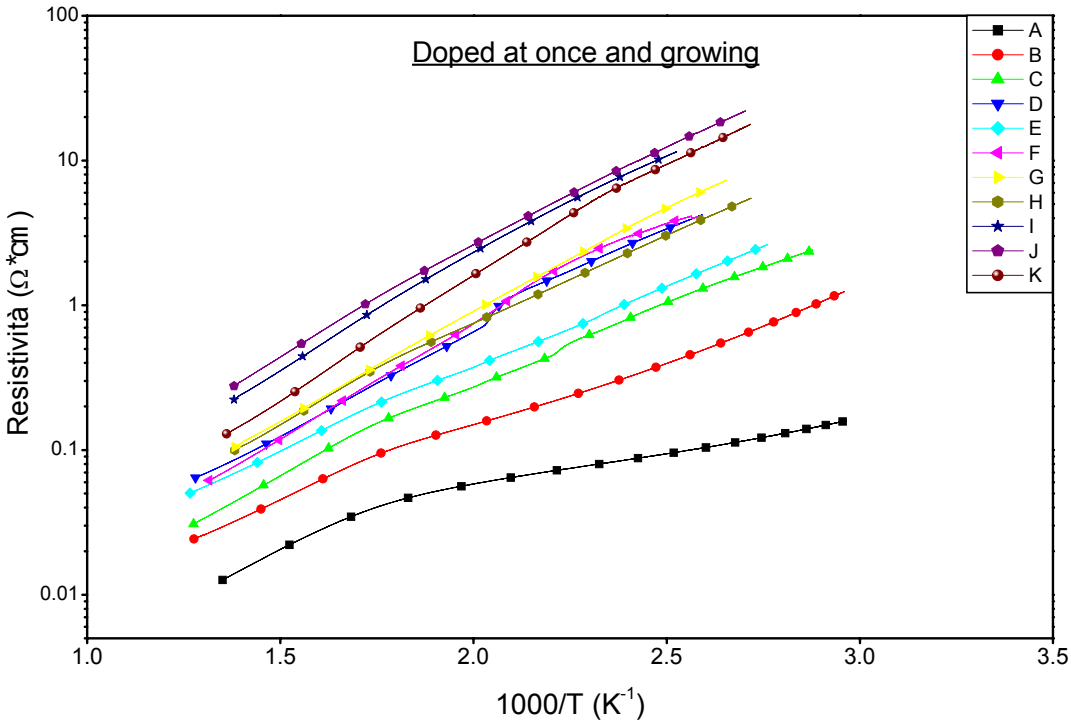

Fig. 3.8 Resistivity as a function of temperature for the so called "*doped at once and growing*" systematic study, in which, the first doped sample is grown with a boron content solution, successive diamond samples were grown only doped by the boron contamination of the chamber of the first sample.

As we can see from these curves, the contaminated growth chamber starts a decontamination process to the time that growths go on, till a remaining contamination that could not be removed, for that reason the only way to reset the chamber to the initial state is to change the quartz tube utilized as reactor. This fact tells us that the contamination of

the chamber occurs on the quartz tube as a form of solid boron deposits that influence following growths. It's noted that the initial boron-doped diamond growths contain a higher doping level, as we can see from the separation of the curves of the first samples; and it's very well note that final samples are concentrated in little doping levels. Nevertheless, it's worth to acknowledge that doping level control is very difficult and only a systematic study of the phenomenon that occur inside the chamber could lighten the physical and chemical dynamics inside the growth chamber. However, besides the random processes that can occur inside the camera, we can have a good idea (through this systematic work) about what happens after an initial boron doped diamond growth and the consequent chamber contamination. Boron concentration was calculated taking into account resistivity at room temperature [81]. It's also important to notice, as we can see from Fig. 3.9(a), that a growing trend of activation energies "E_a" is verified as an inverse function of he doping level. As a matter of fact we can see in Fig. 3.9(b) that resistivity at room temperature increased with decreasing doping level and in Fig 3.9(c) is noted the decontamination process of the chamber, for which, resistivity always at room temperature increases with increasing number of samples grown after the initial contamination of the chamber.

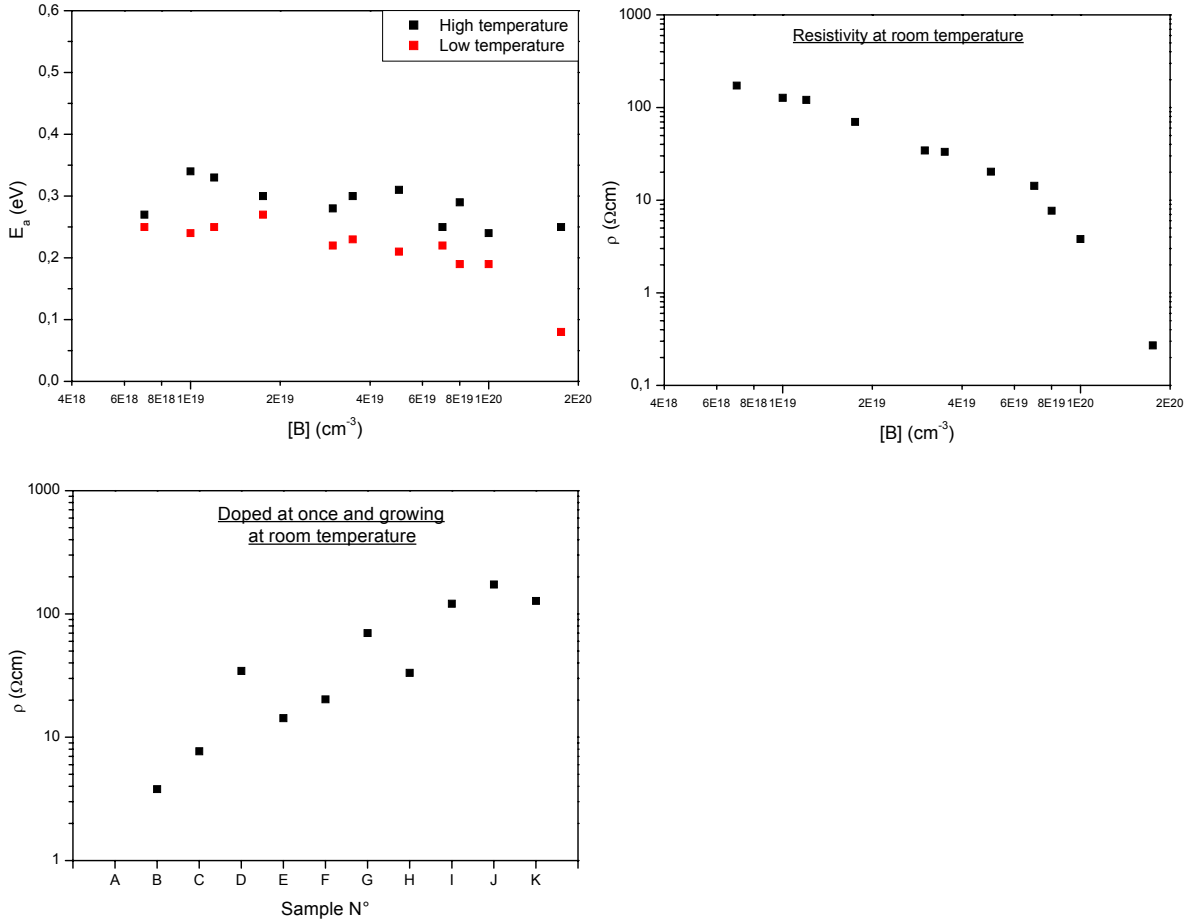

Fig. 3.9 (a) Activation Energy as a function of boron content. **(b)** Resistivity as a function of boron content at room temperature. **(c)** Resistivity as a function of the Nº of sample for "Doped at once and growing" systematic study at room temperature, we can observe a trend in increasing resistivity with the increasing Nº of growths which confirms the decontamination of the camera with successive growths.

3.4.2 Doped at once and growing in presence of methanol systematic study

The purpose of this systematic work is to study how the presence of methanol affects the boron content in boron-doped diamond samples. A first sample Nº L was grown at 0.2 sccm gas flow of boron oxide (1 mg) in methanol (CH_3OH); successive growths were made varying the flow gas of pure methanol (without boron content) in order to establish a systematic behavior that helps to predict how the presence of methanol inhibits diamond doping. The diminishing of doping efficiency for boron may be explained if more and more oxygen is introduced with the doping gas, which mainly consists of methanol.

Leading by plasma reactions inside the chamber, it was found that boron react with oxygen to form boron oxide (B_2O_3), which formed a glassy deposit at moderately hot parts (ca. 500 °C) of the reaction chamber [58]. As we can see from the systematic work described in Fig. 3.10, a doping trend is verified as a function of the content of methanol in the gas flow through the chamber.

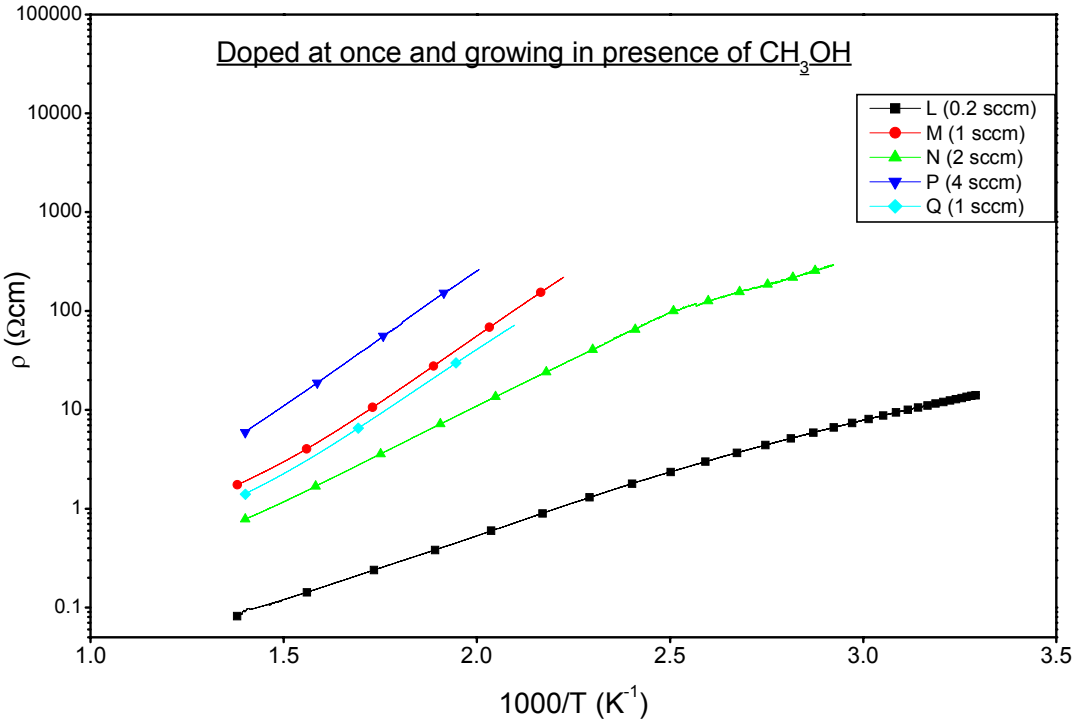

Fig. 3.10 Resistivity as a function of temperature for the so called "*doped at once and growing in presence of CH_3OH*" systematic study, in which, the first doped sample is grown with a boron content solution, successive diamond samples were grown only doped by the boron contamination of the chamber of the first sample but in presence of different methanol contents, which is believed that act as a strong inhibitor of boron doping.

In table 3.1 are summarized the growth conditions of the samples used for the systematic work.

Table 3.1 Sample characteristics used in the present systematic study.

Sample N°	L	M	N	P	Q
CH_3OH flow (sccm)	0.2	1	2	4	1
Activation energy (eV)	0.24	0.39	0.37	0.52	0.48
Doping level (cm^{-3})	$6x10^{19}$	$3x10^{16}$	$3x10^{18}$	$1.7x10^{16}$	$5x10^{16}$
ρ @ 715 K (Ωcm)	0.09122	1.897	0,783	5.903	1.401

From the figure we observe that sample Nº L is the highest doped and it's in concordance with the lowest content of methanol in the gas flow (0.2 sccm), at higher doping contents the experimental behavior of the boron-doped diamond samples follow which is predicted in literature [58], accordingly to the fact that methanol content (because of his oxygen content) act as inhibitor for boron-doped growth. We can also see from the experimental curves that sample Nº Q has higher doping level than sample Nº P because of his lowest methanol content in the gas mix, this fact reinforces the previsions made and shows that there is some degree of control in boron-doping efficiency. Because of this last remark it's worth notice that a very accurate doping control can only be reached by a systematic study under different growth conditions, which in fact, determines an important effort in systematic work to understand all the parameters that must be controlled in order to obtain accurate doping levels. The present work introduces a trend, an approach, to a deep knowledge of the variables to be managed for boron-doped diamond samples in the Mechanical Engineering Department of the University of Rome "Tor Vergata" growth chamber.

It's also worth to notice that the sample Nº L was the sample that contained boron oxide (B_2O_3) in his growth, and it's in the growth of this sample that the camera suffered the contamination of boron and the deposition of glassy deposits; thus, successive samples

were growth without boron content as a solid dopant but only with the contamination of the camera and the presence of methanol, at his different concentrations, that act as doping inhibitor which results in different doping efficiency.

Chapter 4

Piezoresistive effect in boron – doped CVD diamond films

Summary

Nowadays almost every mechanical pressure, force or strain sensor is based on the piezoresistive effect. Theoretically, this effect can be separated into two parts:
1) The geometrical effect that can be found in all conductive materials and semiconductors leading to a change in the electrical resistance of a given resistor due to a change in the geometrical dimensions of the resistor structure owing to an applied external force; and
2) The change of the band structure in a semiconductor, where the lattice is deformed due to an applied external force. The lattice deformation results in a change of the carrier distribution and the average effective carrier mass.
Semiconductor sensors are preferred because the piezoresistive effect is essentially larger due to the change in carrier distribution with respect to their effective mass, and due to their low density as compared to metal-based sensors. Metal-based sensors are mainly used in strain gauges, which only exploit the geometrical piezoresistive effect. Silicon is by far the most popular used semiconductor due to its large piezoresistive coefficients, a well-established fabrication technology and the possibility of monolithic integration of electronic circuits together with mechanical components. However, its suitability is limited due to the weak chemical inertness and poor temperature stability of silicon.
With this general scheme diamond is presented as an attractive sensor material because of its wide bandgap, which may mean that the piezoresistive effect is "hard", that is, it is preserved or even accentuated at high temperatures and radiation conditions (*harsh environment*) that limit conventional materials such as silicon. Furthermore, because intrinsic (undoped) diamond is electrically insulating, it provides an ideal substrate for doped (conducting) diamond patterns and resistors process compatibility. Hence microstructures such as pressure sensors may be created, providing a ruggedness associated with diamond for physical hardness, chemical inertness and thermal conductivity.

4.1 MICROSENSORS

We can define a sensor as an electronic device used to measure a physical quantity such as temperature, pressure or loudness and convert it into an electronic signal of some kind (e.g. a voltage); it means, a sensor transforms a non-electrical magnitude in an electrical one; when measurements systems tended to be large and expensive researchers started to link the microelectronics technologies (see chapter 1) and use these to make silicon sensors, the so-called *microsensors*, then, in particular, a microsensor is a sensor that has at least one physical dimension at submilimeter level. Sensors are normally components of some larger electronic system such as a computer control and/or measurement system.

Analog sensors most often produce a voltage proportional to the measured quantity. The signal must be converted to digital form with a ADC before the CPU can process it.

Digital sensors more often use serial communication such as EIA-232 to return information directly to the controller or computer through a serial port.

We can also define an *actuator* as the converse of a sensor, it means, a device that is capable to transform an electrical signal in a non-electrical response that interacts with surrounding environment; in Fig. 4.1 we can see an information-processing general scheme

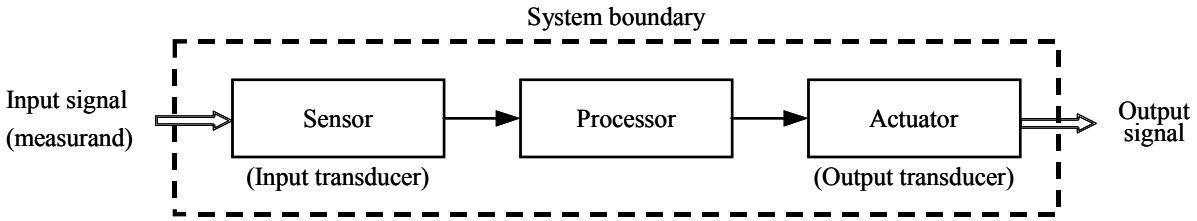

Fig. 4.1 General scheme of an information-processing system.

4.1.1 Sensor response curve

The output response, shown in Fig. 4.2(a), of a given sensor, is the representation of its output as a function of the measurand (object to be measured) applied to its input and it is called sensor response curve. A variety of magnitudes can correctly represent the sensor output response. In the case of a piezoresistor it is recommended to use: $(R - R_0)/R_0$, that is the relative change of resistance, R_0 represents the reference value considered for the normalization.

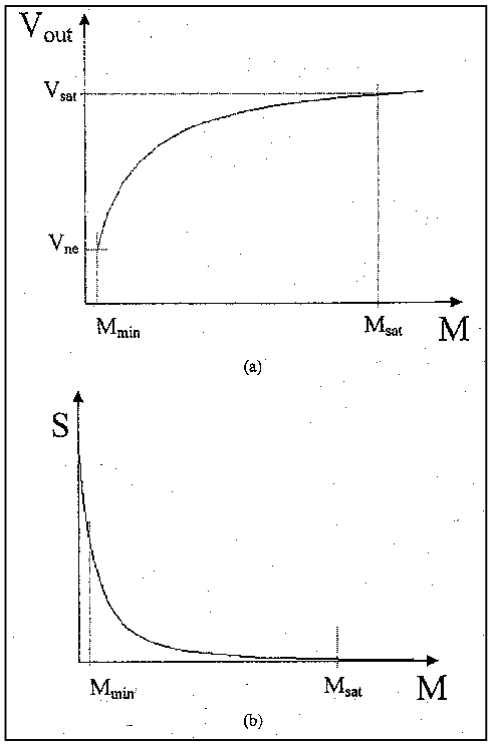

Fig. 4.2 (a) Sensor response curve of generic sensor device. **(b)** Sensitivity of the same sensor device.

The sensor response curve represented in Fig. 4.2, as an example, tell us that the sensitivity approaches to zero for sufficiently high M values and values, different from zero, where its slope is different from zero. In fact in presence of high M values, the output tends to remain constant, which means that the sensor, in this condition, do not react to the input variations.

One can obtain the sensitivity (S) curve by a derivative procedure from the response curve, as represented in Fig. 4.2(b), and the indication along the sensitivity axes must specify the change of the output with respect to the input, in our case, for instance, we have:

$$S = \frac{\partial\left(\frac{R - R_0}{R_0}\right)}{\partial M}$$

All the definitions based on the output/input derivative are always valid, simply because sensors are, generally, non-linear in character but can be simplified in those cases where the degree of non-linearity can be neglected.

4.1.2 Internal sensitivity (^iS)

By this term, which deserves some attention, we intend the degree of reaction of a given sensitive material property (X), with respect to a measurand change that can be infinitesimal, finite or total. According to the input measurand change, ^iS may be represented in three ways: $\partial X/\partial M$, $\Delta X/\Delta M$, X/M, in the cases of nonlinear, linear with offset and linear without offset behavior respectively.

The offset, which can also be time dependent, can come by some memory and aging effects, unbalancing of differential stages of the preamplifier and amplifier, or even by the measuring technique.

^iS does really represent a meaningful parameter useful for the comparison among similar kinds of sensors with respect to the same measurand, or even with respect to different types of measurand. In this last case, it is worth considering different internal sensitivities, each referred to one type of measurand.

$$ {}^{i}S_j = \begin{cases} \dfrac{\partial X}{\partial M_j} \\ \dfrac{\Delta X}{\Delta M_j} \\ \dfrac{X}{M_j} \end{cases} \qquad j = 1,\ldots, n \text{ (}n\text{: number of measurands)} $$

The dependence of internal sensitivities on the possible measurand may be rather complex if we take into consideration the fact that interference among measurands is possible as well interference on the internal sensitivity mechanisms of the sensing material. A measurand could be affected from different unwanted quantities such as: relative humidity (*RH*), pressure (*p*), time (*t*) and so on; as a consequence and in our particular case, one of the internal properties, such as resistivity ρ, can be expressed as a function of non-independent quantities $\rho = f(M, RH, p, t, \ldots)$ through a Taylor expansion.

Fortunately, in most of the practical cases, we do not have to deal with all these terms or it is possible to create operative conditions for the sensor, in order to avoid them. Thus, the expression of the resistivity can be greatly simplified to include only linear terms and, due to the intrinsic noise level, most of the cross-term coefficients of the Taylor expansion can be considered small enough to be neglected.

4.1.3 Resolution, noise and drift

Due to the unavoidable fluctuations of chemical, physical, and biological quantities, any property of a given sensing material experiences fluctuations that represent the origin of the electrical noise, evaluated as the root mean square value of the fluctuations. Sensors, whatever their complexity may be, manifest noise at their output with a given signal to noise ratio. This noise is one of the reasons that the resolution cannot approach the zero value; another direct reason is the sensitivity value limitation.

Different kind of noise may be present, even if not simultaneously, in a given sensor, such as Johnson (thermal), shot, generation recombination (g-r), contact, $1/f$ (flicker) noise [59].

Certainly, without the knowledge of the noise level, it is not possible to estimate the resolution. The resolution is obtained through a limit procedure and the relationship is reported in Eq. 4.1 for a further consideration in its general form.

$$\text{resolution} = \lim_{V_s \to V_{noise}} \frac{V_s}{S} = \frac{V_{noise}}{S} \tag{4.1}$$

It is worth pointing out that, in a nonlinear transfer function, the sensitivity S and the noise level are functions of the operating point (o.p.) and so is the resolution. As a consequence, it appears that is not correct to specify the resolution of a given sensor, as it frequently appears in literature, without the accurate specification of its o.p.

Concerning the drift, we can define it as a slow unpredictable change of the sensor output, undefined from the statistical point of view, which is superimposed to both the signal and noise levels. Its origin may be correlated to the aging of the sensing material (release of internal stresses, slow residual diffusion processes) and of the electronic components that interact with chemical, physical, and biological quantities present in the environment. Its presence can be detected usually through a long time observation and can be considered another reason of the loss of accuracy of the sensor.

A rather satisfactory shrewdness consists in using sensors having response time as low as possible and in controlling both the zero level stability at the output and the calibration state.

4.2 BAND THEORY OF PIEZORESISTIVE EFFECT

Based on studies of the energy-band structure of diamond [60,61], a simplified band diagram of the diamond valence band is shown in Fig. 4.3(a) for zero stress. The heavy-hole band with an effective mass $m_{hh}^{*} = 218m_0$ and the light-hole band with an effective mass $m_{lh}^{*} = 0.7m_0$ [61] are degenerated at $k = 0$, where m_0 is the free electron mass. The split-off band, with an effective mass $m_{sh}^{*} = 1.06m_0$, is separated from the degenerate bands only by ≈ 5 meV due to spin-orbit interaction. Since the separation is small, the valence band is nearly triply degenerate in energy. Since the valence structures of p-type silicon and diamond are similar to a certain degree, the discussion of the former can be extended carefully to the latter.

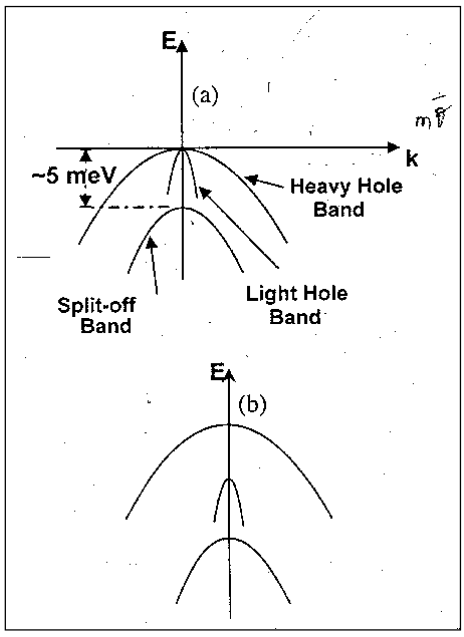

Fig 4.3 Simplified band diagram of the diamond valence band for: **(a)** Zero stress and **(b)** Uniaxial positive stress (tension).

In the case of Si, the energy separation between the degenerate bands and the split-off is 44 meV and is usually neglected in the discussion of stress-induced changes in the valence band. Following a similar discussion for diamond, it is assumed that, for a

qualitative discussion, only the changes in the heavy and light-hole bands play a dominant role in the stress-induced change of the sensitivity of diamond.

When an uniaxial positive stress (tension) is applied in the longitudinal direction, the heavy-hole band E_{Vhh} moves up relative to the light-hole band E_{Vlh} (Fig. 4.3(b)). This results in an increase in the number of heavy holes and a decrease in the number of light holes. Consequently, the resistivity increases. The compressive stress (negative) causes the light-hole band to move up with respect to the heavy-hole band, resulting in a decrease in resistivity.

In the above discussion, only the relative shifting of sub-bands is considered. The direct changes in effective mass may also occur if the stress causes a change in the curvature of the sub-bands. Stress-induced changes in the band gap, seem less likely because of the large band gap (5.5 eV) of diamond. Since in the case of diamond the split-off band is separated from the degenerate bands only by ≈ 5 meV, and the effective mass is not small, the effect of uniaxial stress on the split-off sub-band may be appreciable.

4.2.1 Numeric approach of piezoresistive effect

In a material subjected to stress X_{kl} the electric field E_i is a function of the current density J_j and stress X_{kl} [62-64]:

$$E_i = \rho_{ij} J_j + \pi_{ijkl} J_j X_{kl} \qquad i,j,k,l = 1, 2, 3 \qquad (4.2)$$

where ρ_{ij} is the resistivity and π_{ijkl} is the piezoresistive tensor. In the case of crystals with cubic symmetry, such as diamond and silicon, π_{ijkl} is given by [62]:

$$\pi_{ijkl} = \begin{cases} \rho_0\pi_{11} & \text{if both J and X are in } [100] \text{ directions} \\ \rho_0\pi_{12} & \text{if J and X are in } [100] \text{ directions but are perpendicular to each other} \\ \rho_0 \dfrac{\pi_{44}}{2} & \text{for shear stress} \end{cases} \quad (4.3)$$

where π_{11}, π_{12} and π_{44}, are the fundamental longitudinal, transverse and shear piezoresistive coefficients, respectively, and ρ_0 is the zero-stain resistivity [65]. For the longitudinal case, Eq. (4.2) can be written as:

$$E_i = \rho_0 J_1 + \rho_0 \pi_{11} J_1 X_1 = \rho J_1 \quad (4.4)$$

where the subscript 1 denotes the [100] direction, and

$$\rho = \rho_0 + \pi_{11}\rho_0 X_1 \quad (4.5)$$

Eq. (4.5) gives:

$$\frac{\rho - \rho_0}{\rho_0} = \pi_{11} X_1 \quad (4.6)$$

In arbitrary directions Eq. (4.2) can be expressed in terms of the fundamental piezoresistance coefficients and the direction cosines. For the longitudinal case, Eq. (4.2) can be written as [62-64]:

$$E_1' = \rho_0 J_1' + [\pi_{11} - 2(\pi_{11} - \pi_{12} - \pi_{44}) \times (l_1^2 m_1^2 + l_1^2 n_1^2 + m_1^2 n_1^2)]\rho_0 J_1' X_1' = \rho_1' J_1' \quad (4.7)$$

where:

$$\rho_1' = \rho_0 + \rho_0 \pi_l X_1' \quad (4.8)$$

with:

$$\pi_l = \pi_{11} - 2(\pi_{11} - \pi_{12} - \pi_{44})(l_1^2 m_1^2 + l_1^2 n_1^2 + m_1^2 n_1^2) \quad (4.9)$$

Eq. (4.8) yields:

$$\frac{\rho_1' - \rho_0}{\rho_0} = \pi_l X_1' \quad (4.10)$$

The primed quantities refer to an arbitrary direction, and l_i, m_i and n_i ($i = 1, 2, 3$) are the direction cosines of the transformation. Similarly, for the transverse case, it can be shown that:

$$\frac{\rho_1^{'} - \rho_0}{\rho_0} = \pi_t X_2^{'} \tag{4.11}$$

where π_t, the transverse piezoresistance coefficient, is given by:

$$\pi_t = \pi_{12} + (\pi_{11} - \pi_{12} - \pi_{44})(l_1^2 l_2^2 + m_1^2 m_2^2 + n_1^2 n_2^2) \tag{4.12}$$

The most suitable and practical quantity in microsensor applications is the piezoresistive gauge factor (GF), which is normally measured, and is defined by:

$$GF = \frac{\Delta R}{R}\frac{1}{\varepsilon} \tag{4.13}$$

For isotropic materials it can be written as [62]:

$$GF_{il} = \frac{\Delta\rho}{\rho_0}\frac{1}{\varepsilon_l} + 1 + 2\nu \tag{4.14}$$

for the longitudinal direction, and

$$GF_{it} = \frac{\Delta\rho}{\rho_0}\frac{1}{\varepsilon_l} - 1 \tag{4.15}$$

for the transverse direction. In the above equations ν, ε_l and ρ are the Poisson's ratio, longitudinal strain and resistivity, respectively, and $\Delta\rho = \rho - \rho_0$. The subscripts i, l and t refer to isotropic, longitudinal and transverse, respectively.

For an anisotropic homogeneous material, the gauge factor is given in terms of the compliance coefficients S_{11}, S_{12} and the longitudinal piezoresistance coefficients π_l by [62]:

$$GF_{al} = 1 - 2\frac{S_{12}}{S_{11}} + \frac{\pi_l}{S_{11}} \tag{4.16}$$

For diamond, $S_{11} = 0.09493 \times 10^{-12}$ cm^2 dyne^{-1}, $S_{12} = 0.00978 \times 10^{-12}$ cm^2 dyne^{-1} (monochrystalline diamond), $\nu \approx 0.07$ and Young's modulus $Y = 11.43 \times 10^{12}$ dynes cm^{-2} (1143 GPa, polycrystalline diamond) [66-68] and Eqs. (4.14), (4.15) and (4.16) can be written as:

$$GF_{il} = \frac{\Delta\rho}{\rho_0}\frac{1}{\varepsilon_l} \tag{4.17}$$

$$GF_{it} = \frac{\Delta\rho}{\rho_0}\frac{1}{\varepsilon_l} - 1 \tag{4.18}$$

$$GF_{al} = \frac{\pi_l}{S_{11}} \tag{4.19}$$

The anisotropic transverse gauge factor can be written as:

$$GF_{at} = \frac{\pi_t}{S_{11}} \tag{4.20}$$

For randomly oriented polycrystalline films the longitudinal piezoresistive coefficient can be estimated by averaging π_l in Eq. (4.9) over all possible directions and is given by [69]:

$$\langle \pi_l \rangle = \frac{\int_{\theta=0}^{\theta=\pi/2}\int_{\phi=0}^{\phi=\pi/4} \pi_1 d\theta d\phi}{\int_{\theta=0}^{\theta=\pi/2}\int_{\phi=0}^{\phi=\pi/4} d\theta d\phi} \tag{4.21}$$

where θ and ϕ are the angles between the arbitrary coordinate system and the principle coordinate system aligned with the crystal axes. For randomly oriented polycrystalline

diamond films, $\langle \pi \rangle$ can be found by making use of Hooke's law and Eqs. (4.10), (4.11), (4.17), (4.18) and (4.21):

$$\langle \pi_l \rangle = GF_{il} \frac{1}{Y} \tag{4.22}$$

$$\langle \pi_t \rangle = GF_{it} \frac{1}{Y} \tag{4.23}$$

In the case of monochrystalline diamond films π_l and π_t are given by [70,71]:

$$\pi_l = S_{11} GF_{al} \tag{4.24}$$

$$\pi_t = S_{11} GF_{at} \tag{4.25}$$

4.3 OPPORTUNITIES FOR DIAMOND AS A PIEZORESISTIVE SENSOR

Diamond is a promising material for new semiconductor devices because of its unique electrical properties. Diamond based sensors operating as termistors and piezoresistors are uniquely suited to chemically harsh, high-radiation and high-temperature environments; due to this fact, in this part of the present work are reported some developments made from different research groups in order to enlighten opportunities for diamond-based devices apt to be develop in concrete applications in science and industry.

4.3.1 Diamond-based strain gauges

An undoped insulating polycrystalline diamond layer, deposited on a silicon wafer (diamond/Si), was used as a substrate for deposition of B-doped polycrystalline CVD diamond films [72]. The thickness of the deposited p-type CVD diamond layer was 1-2 μm.

P-type diamond strain gauge were fabricated by etching the B-doped CVD diamond films deposited on the substrate. The length and the width of the strain gauge path were 500 μm and 50 μm respectively. A schematic representation of the fabricated p-type CVD diamond strain gauge pattern is shown in Fig. 4.4.

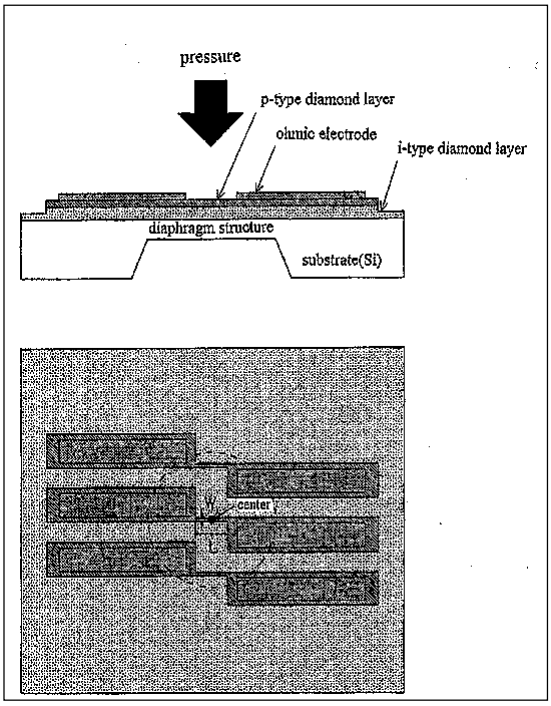

Fig. 4.4 CVD Diamond-based strain gauge structure.

The p-type polycrystalline CVD diamond strain gauge, fabricated on the diamond/Si diaphragm, was placed in a special test chamber to measure the piezoresistive effect. Argon gas was introduced into the chamber in order to apply a positive gas pressure (up to 10 Mpa) against the sealed diaphragm structure. The amount of strain ε produced in the diamond strain gauge was proportional to the applied gas pressure, and reached about 30 microstrains at a gas pressure of 10 Mpa.

A large piezoresistive effect was observed in the p-type diamond strain gauges when a compressive stress was applied by increasing the gas pressure. The gauge factor (*GF*) of

the p-type polycrystalline diamond was estimated to be about 1000 at room temperature, and remained above 700 even at 200 °C. The very large gauge factor of the p-type CVD diamond films offers the promise of a sensitive piezoresistor suitable for use in pressure and acceleration sensors operating in chemically harsh, high-radiation and high-temperature environments.

4.3.2 Diamond-based pressure sensors

PZR-based pressure sensors can be derived from micromechanical diaphragm structures [73]. This configuration can be achieved in diamond because Polycrystalline Diamond Films (*PDF*) piezoresistors can be directly patterned on undoped diamond diaphragms. There are two advantages in using PDF as the diaphragm material. First, PDF is chemically inert and can serve as an etch-stop with large etching time tolerance. Second, PDF can be deposited with control by adjusting deposition time and other grow parameters, resulting in selectability of diaphragm thickness. Therefore the full-scale pressure range can be varied with PDF as the diaphragm material. The sensitivity of diaphragm sensors depends on a variety of parameters, such as the diaphragm size, the impurity doping concentration and the gauge location. Resistor placement on a diaphragm can be chosen to achieve maximum strain and optimize the PZR effect.

The stress pattern due to pressure difference across a diaphragm is known [73]. The radial strain in the diaphragm is:

$$\varepsilon_{rr} = \frac{3P(1-\nu^2)}{8Et^2}\left(R_0^2 - 3r^2\right) \tag{4.26}$$

where R_0 is the radius of the diaphragm, P is the pressure difference, t is the thickness and v is Poisson's ratio, which is 1 to 2 for diamond. The tangential stress can be expressed as:

$$\varepsilon_{\theta\theta} = \frac{3P(1-\nu^2)}{8Et^2}\left(R_0^2 - r^2\right) \qquad (4.27)$$

The radial and tangential strains have the same magnitude in the center. There are tensile stresses at the edges and compressive stress in the center.

Polycrystalline diamond films for the pressure sensor were grown using a microwave plasma-enhanced chemical vapor deposition system. The average growth rate was nominally 0.5 microns per hour. The p-type boron doped PDF piezoresistors were fabricated on undoped diamond films via in situ boron solid source doping method. The resistors were doped during deposition with boron from a solid wafer boron compound source, which was placed under the substrate during resistor deposition. Boron outgases at the processing temperatures and is incorporated into the growing diamond film [73]. Four resistors (width = 0.5 mm) are positioned on top of the diaphragm. Two resistors (R1, R2) have their lengths oriented radially to examine longitudinal PZR, and the other two resistors (R3, R4) have their lengths orthogonal to the radius to examine transverse PZR. The diaphragm thickness was 5 microns, diameter 0.92 cm and the doped diamond resistor was approximately 3 microns thick. The diaphragm was highly insulative (>1 GΩ) as determined by *I-V* measurements at room temperature.

A differential pressure was produced on a specially designed fixture to examine the PZR effect of these diamond resistors. Pressure was applied to the membrane in the range 0-250 mm Hg. The resistances of the four resistors were taken individually at varying pressures. As a result the resistance changes of the two longitudinal PZRs, identified as R1 and R2, are larger than those of the other two transverse resistors, R3 and R4. R1 has a piezoresistance of 0.1% per 100 mm Hg and R2 has a slightly lower response. This is due to a slight asymmetry of this particular device, where more length of R1 is on the membrane than R2. R3 and R4 have a diminished PZR as they are in the transverse

configuration. As a conclusion, the PZR effect in diamond can be used to make a functioning electronic pressure microsensor and can be readily extended to other microsensor configurations, such as accelerometers and microswitches. The PZR effect is function of the doping level and other PDF properties such as grain size and deposition conditions.

4.3.3 Diamond-based accelerator

Cantilevers with integrated piezoresistors are a basic test structure for mechanical properties. However, most data on piezoresistive sensor devices are not reported on cantilevers but on full membranes. In the present description [74] macroscopically stress-free films have been demonstrated and processed into 15 μm thick cantilevers with piezoresistors integrated at the root of the structure [75]. The following properties have been identified: a Young's modulus of $E = 825$ GPa and a fracture strength of up to 4.7 GPa. At this strength, although only approximately half of the ideal value, the fracture through the polycrystalline beam follows already in part the (111)-plane, which is the diamond cleavage plane [76]. These data have been obtained by resonance frequency and nano-indentation measurements. The gauge factor of the piezoresistor is dependent on the doping concentration and at moderate thermal activation (and therefore moderate sheet resistance at room temperature), a gauge factor of $K = 8$ is seen up to the full fractures strength. No hysteresis and thus no regime of plastic deformation is observed in a stress-cycling and holding experiment [75].

Based on these data as a first demonstrator, an acceleration sensor using an Si-seismic mass in the center of a square shaped diamond membrane, which has then been patterned into a fourfold bridge, has been designed and fabricated. The signal is read out by a Wheatstone bridge. Two resistors are located at the beam ends and two outside the

suspended structure. The chip has then been mounted into an experimental test setup, and subjected to a single shock and vibration test on a mechanical shaker. An output signal amplitude of ± 150 mV is detected decaying within seconds, mainly caused by atmospheric attenuation. In the decay transient, the first resonance can also be identified, which is 4.5 kHz. Both the deflection of the seismic mass and the ground state resonance frequency have been simulated using a commercial finite element program, where the resonance was found to be in good agreement with the experiment, with $f_{res} = 4.7$ kHz. With a fracture strength of 4.5 GPa, destructive failure is predicted at an acceleration of 7×10^3 G. Experimentally, no deterioration has been observed up to an acceleration of 40 G, the limit of the test setup. The predicted strength of these structures is extremely high. In addition, the Young's modulus and the fracture strength should not degrade for operating temperatures up to at least 700 °C in atmosphere, where the unpassivated films start to erode [77]. First applications may therefore be expected in extreme and hostile environments. Then the Si-substrate may limit the performance above 500 °C and an alternative substrate like cubic SiC will be needed.

Chapter 5

Experimental setup of piezoresistive effect demonstrator

Summary

MEMS pressure microsensors typically have a flexible diaphragm that deforms in the presence of a pressure difference. The deformation is converted to an electrical signal appearing at the sensor output. A pressure sensor can be used to sense the absolute air pressure within the intake manifold of an automobile engine, so that the amount of fuel required for each engine cylinder can be computed. In this example, piezoresistors are patterned across the edges of a region where a silicon diaphragm will be micromachined. The substrate is etched to create the diaphragm. The sensor die is then bonded to a glass substrate, creating a sealed vacuum cavity under the diaphragm. The die is mounted on a package, where the topside of the diaphragm is exposed to the environment. The change in ambient pressure forces the downward deformation of the diaphragm, resulting in a change of resistance of the piezoresistors. On-chip electronics measure the resistance change, which causes a corresponding voltage signal to appear at the output pin of the sensor package [78].
This work is intended to develop a demonstrator capable to show piezoresistive effect on boron-doped diamond films grown at the Mechanical Engineering Department of the University of Rome "Tor Vergata" laboratories. For that scope, it was developed an *ad-hoc* device in order to manifest the mentioned effect. Nevertheless, our study will be centered in qualified and quantified the piezoresistive effect in order to evaluate Boron-doped diamond as a strain gauge material, we desire that the work develop in the PhD period serve to enlighten future studies and a deeper knowledge of the diamond properties with the final scope to interact with industrial partners in order to realize a diamond based sensor.

5.1 DEMONSTRATOR APPARATUS DESCRIPTION

In order to evidence piezoresistive effect a demonstrator apparatus was realized at the Mechanical Engineering Department of the University of Rome "Tor Vergata" laboratories, this apparatus was designed in order to qualify piezoresistive effect of the boron-doped CVD diamond films grown at the mentioned laboratories at different temperatures and different strain values. A general scheme of the apparatus is shown at Fig. 5.1.

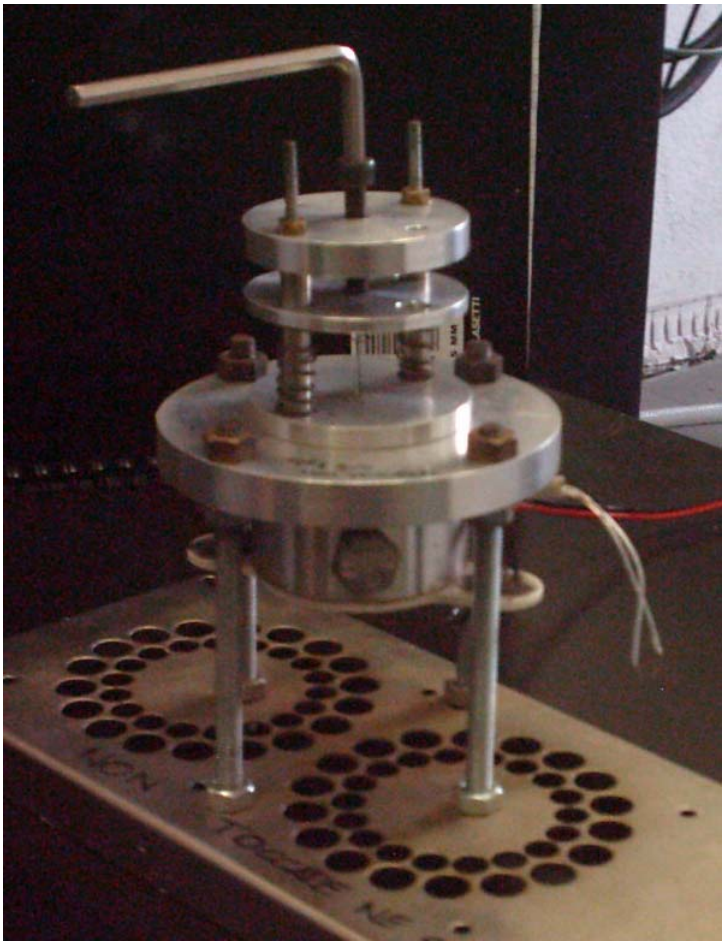

Fig. 5.1 General scheme of the apparatus to put in manifest piezoresistive effect.

In order to realize measurements with varying temperature, a heater was placed under the metallic container which allows a range of temperature from T_{amb} till 200 °C, which is the maximum temperature measurements, moreover as it is shown in next chapter, the

systematic study was performed at T_{amb}, 50, 100, 150 and 200 °C. The diamond sample are placed face "*down*" in the apparatus, then, cupper supports act as physical support and contacts in order to transmit the signal out from the apparatus. Gold contacts on the sample were evaporated in order to achieve high quality and high adherence contacts on the sample surface, then, they were "stick" on the sample support through silver paint in order to connect sample contacts with the read-out signal line. The upper part of the sample is the silicon substrate which is exposed to the force actuator, which is in essence, a spring with a round extreme which transmits the force to the silicon substrate. The application of the force on the silicon substrate placed in a bridge configuration generates the strain ε of the diamond sample, giving place to a tension stress state in the diamond film as we will see in next chapter. In order to evaluate the applied force, the system was calibrated in a scale to measure accurately the force level of the system in bridge configuration.

Having the load level we can calculate the strain value through the following formula:

$$\varepsilon = \frac{3W(2d-a)}{4Et^2b} \tag{5.1}$$

Where W is the applied load (*force*), d the distance between supports, a the distance between contacts, E the Young's modulus, t the thickness and b the sample wide.

5.1.1 Force application system

In order to calibrate the applied force on diamond samples the system was calibrated through an analytic scale (Sartorius Mod. A210P) to accurately obtain load values, as we can see in Fig. 5.2 the applied load is linear consequently with the force produced by a spring.

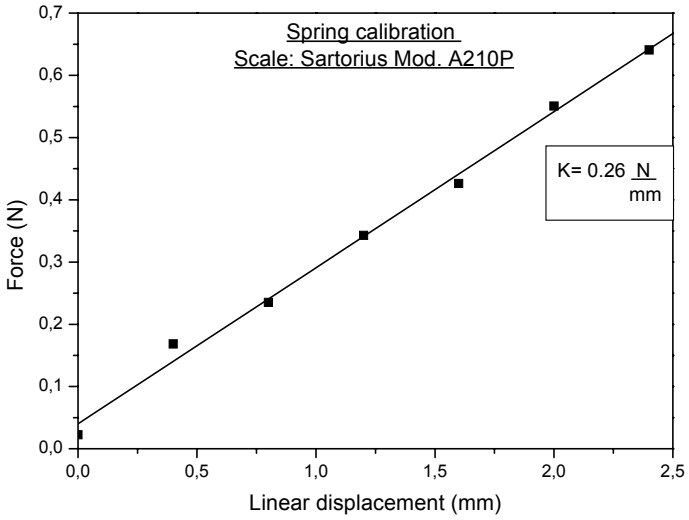

Fig. 5.2 Graphic of the load curve used in the calibration of the force application system.

This load values will be used to calculate the strain value through eq. (5.1), then this values of strain will allow to calculate an important parameter for the piezoresistive effect that is the "*gauge factor*".

5.1.2 Thermal regulation

Temperature measurements of the piezoresistive response were performed on the same apparatus for which is mandatory an accurate thermal regulation. In order to obtain high temperatures a heater was placed on the bottom of the system, at it is shown in Fig. 5.1; the heater is in essence a resistance which profits Joule's effect to heat the apparatus. To accurate measure the temperature a termistor (RS PT100 class A) was placed inside the chamber and near the sample, the temperature measured by the termistor was transformed in temperature through the following algorithm:

$$T = \frac{R_t - R_0}{AR_0} \tag{5.2}$$

Where R_t is the resistance measured by the multimeter, R_0 is the reference resistance of the instrument at 0 °C (100 Ω), A is the linear parameter of the termistor ($3.9083*10^{-3}$); because the following term is four orders of magnitude lower it can be neglected.

Due to the reduced space of the chamber we can say that the temperature reached inside is homogeneous and temperature gradients can be neglected. The acquisition system allows to acquire the temperature through resistance measurements made by a multimeter (Keithley 2000) and by this acquisition system perform the thermal regulation of the system.

The main idea was to maintain the temperature in the range ± 0.05 °C, that's the reason for which real time acquisition of the temperature was mandatory. It is worth note that a low temperatures some diamond samples (specially those of low doping level) are very sensible to temperature changes and an error in temperature control could hide the studied effect and introduce errors due to a R(T) measurement instead a piezoresistive effect.

5.2 ACQUISITION SYSTEM

Piezoresistive effect on CVD boron-doped diamond films, grown at the Mechanical Engineering Department of the University of Rome "Tor Vergata" laboratories, was measured through the characteristic *I-V* of the material, contacts were made at it is shown in Fig. 3.6. For this purpose an acquisition system is described in the scheme of Fig. 5.3.

Fig. 5.3 Photograph of the acquisition data system where it is shown the demonstrator apparatus, the DC Power supply used for temperature measurements and the multimeters that read the signal from the apparatus and transmitting them to the computer for control and analysis.

In this scheme we can see three multimeters, the Keithley 6517A which is the multimeter used for the *I-V* characteristic, this multimeter allows to read high resistance (electrometer) and has its own programmable voltage source which made it ideal for this type of measurements. The other multimeter, Keithley 2000, it's a standard multimeter that reads the resistance of the termistor inside the piezoresistive apparatus in order to know the apparatus inside temperature; the third one is another Keithley 2000 use to calibrate by comparison of resistance measurement the previous one. This three multimeter are connected through GPIB cards and cables to a computer, then, an "*ad-hoc*" Quick Basic® program, that take the signal from the multimeters, compute and graphic real time results for visualization. Logically the acquired data are saved for further analysis.

Chapter 6

Time response of boron – doped CVD diamond films

Summary

An important aspect in acquisition data is the fact that between different measurements a pause must be set in order to allow the system to reach a steady state able to be measured by the acquisition data system. Because of, we are varying the applied voltage (through a programmable voltage source) in order to make *I-V* characteristic, current fluctuate until it arrives to the mentioned steady state. This state is not immediately reached and depends on different factors as temperature, strain and doping level in which resistivity is implicit. Without this steady state we won't be able to accurately measure piezoresistive effect then we would introduce high errors level. As we said before, a pause must be established, in order to do that, time response studies were made and a pause time fixed for the different samples that are under analysis.

6.1 I-V CHARACTERISTIC

In this chapter we will focus on the study of time response of diamond as a result of the application of a variable voltage to the diamond sample by a programmable voltage source (Keithley 6517A) that allow to read different current levels depending on resistivity, this behavior is illustrated in the *I-V* characteristic (see Fig. 6.1(a)). The *I-V* characteristics in different conditions are the main measures to be done because it clearly shows the different effects that we want to put in evidence (i.e.: Doping level, Gauge factor, $\Delta R/R$, temperature dependence). The change in the applied voltage causes a delay in reaching the steady state (DC) values, in order to avoid this delay and to read an accurate current value, a pause must be set; for that, measures of current as a function of time *I(t)* were done in order to established when diamond samples reaches the steady state and are ready to data acquisition for different temperatures at the same power applied. The time in which the system reaches the steady state will be set as "the pause" of the system for data acquisition. If we don't established a pause time and we continuously acquire data an "apparent" hysteresis effect it's produced between increasing voltage values and decreasing voltage values at it is shown in Fig. 6.1(b). It's clearly notice the relation between hysteresis effect and the delay in reaching the steady state, for that, setting a pause and reaching the current steady state the hysteresis effect it's almost eliminated as we can see in Fig. 6.1(b). Moreover, temperature studies of time delay and applied strain will be performed in order to established one pause value that will be take as a fixed parameter in data acquisition. The systematic study is complete introducing the applied strain and doping level in time response.

6.2 APPARENT HYSTERESIS EFFECT ON DATA ACQUISITION PAUSE

This subchapter focuses on the hysteresis effect found on *I-V* measurements that directly affects the mentioned steady state and conditioned the selected pause established for our measurements. In Fig. 6.1 we can see two graphics that put in evidence the mentioned hysteresis effect on the measure, this measure was made at room temperature.

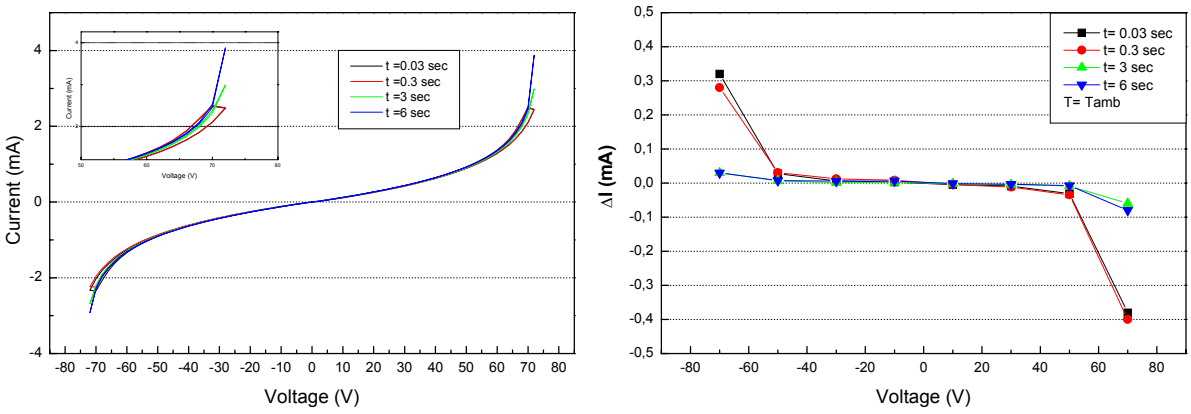

Fig. 6.1 (a) *I-V* characteristic for different acquisition pause and zoom in the apparent hysteresis zone. **(b)** ΔI due to apparent hysteresis effect as a function of voltage and acquisition pause.

We can see in Fig. 6.1(a) the *I-V* characteristic of a diamond sample in which is clearly show the hysteresis effect for the different curves depending on pause time, as we can see this effect diminished for increasing pause time between successive acquisitions. Fig 6.1(b) show the current variation (i.e.: the hysteresis effect) Δ*I* between increasing voltage step and decreasing voltage step for different pause time at room temperature; it is worth noting that the effect diminish for increasing pause time between acquisitions as we conclude before. This analysis is very useful because this effect, combined with the above mentioned steady state, will allow the selection of time pause that we will use for all our measurements and for all the analysis made for B-doped diamond samples as piezoresistors. Established this concepts let see what happened with current when we apply a voltage at room temperature.

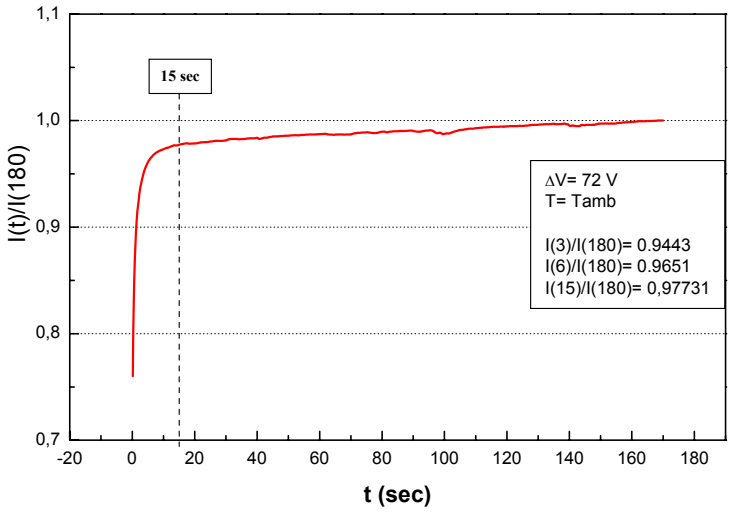

Fig. 6.2 Time response of diamond at room temperature normalized at 180 seconds.

In Fig. 6.2 it is shown the time response of diamond at room temperature normalized at 180 seconds, it's shown that at 15 seconds it's reached almost the 98% of the signal, and we can say that it is reached the steady state.

6.3 EFFECT OF TEMPERATURE IN TIME RESPONSE

In Fig. 6.3 it's shown a graphic of a diamond sample for different temperatures. In these curves, that are normalized to the value at 15 seconds, it's clearly show that time response decrease at increasing temperatures (maintaining power at a constant value of 150 mW), then the situation improves with increasing temperature.

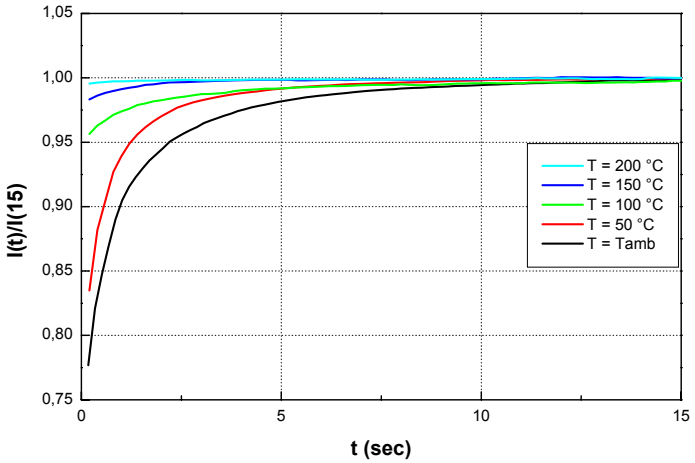

Fig. 6.3 Graphic of time response for different temperatures, it is clearly show the decreasing time response with increasing temperature.

A proper explanation could be found through the change of resistivity with temperature, in which the effective mass (m*) is taken as a parameter that depends on temperature [79], that causes changes in the carriers number [80] which is macroscopically verified by the change in the time response.

6.4 EFFECT OF THE APPLIED STRAIN IN TIME RESPONSE

Another important effect to be evaluated is the applied strain on the time response of the sample under studying. As we can see in Fig. 6.4 there are some differences between the time response for different applied strain, the percentage variation at t = 4 sec (where is verified the maximum gap between the minimum and maximum applied strain) is 4%; then, we can observe from Fig. 6.4 that time response decrease with increasing strain.

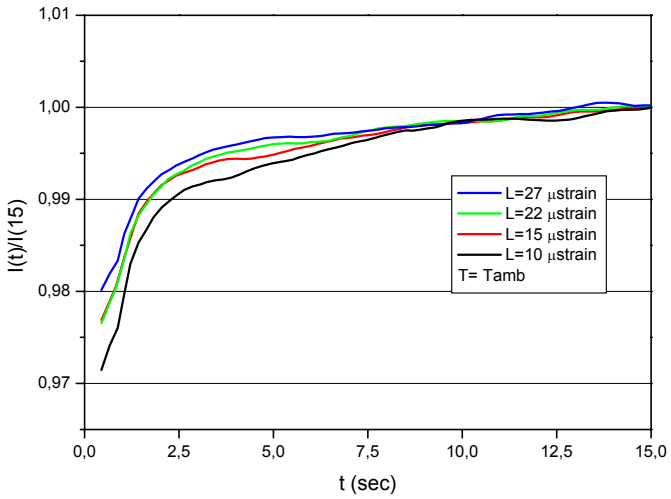

Fig. 6.4 Graphic of time response for different applied strain, it is clearly show the decreasing time response with increasing applied strain.

Thus, we can say that diamond response at lower strain is slower, the other one are similar each other when diamond sample is subjected to an increasing strain level.

The explanation of this phenomenon could be approached in the following direction, the strain that made changes in the heavy hole and light hole bands (degenerated from the valence band, see chapter 4.2) causes changes in the carriers type involved in electrical conduction [61], thus difference in the resistivity that is verified by means of different time response from CVD diamond samples with different applied strain levels.

6.5 TIME RESPONSE AS A FUNCTION OF TEMPERATURE AND DOPING LEVEL OF B-DOPED CVD DIAMOND FILMS

In this chapter the combined effect of temperature and doping level is studied in order to enlighten possible devices setup in order to build a piezoresistive strain gauge. In order to clarify in Table 6.1 it is shown the different doped diamond samples used in experimental measurement.

Table 6.1 Doping level for different diamond samples used in experimental measurements.

Sample	N° 1	N° 2	N° 3	N° 4	N° 5	N° 6
Doping level (cm^{-3})	$6x10^{19}$	$2.7x10^{19}$	$1.75x10^{19}$	$5x10^{18}$	$3x10^{18}$	$1.7x10^{16}$

In Fig. 6.5 it is shown three graphics for three different samples: N° 2, N° 3 and N° 6 respectively.

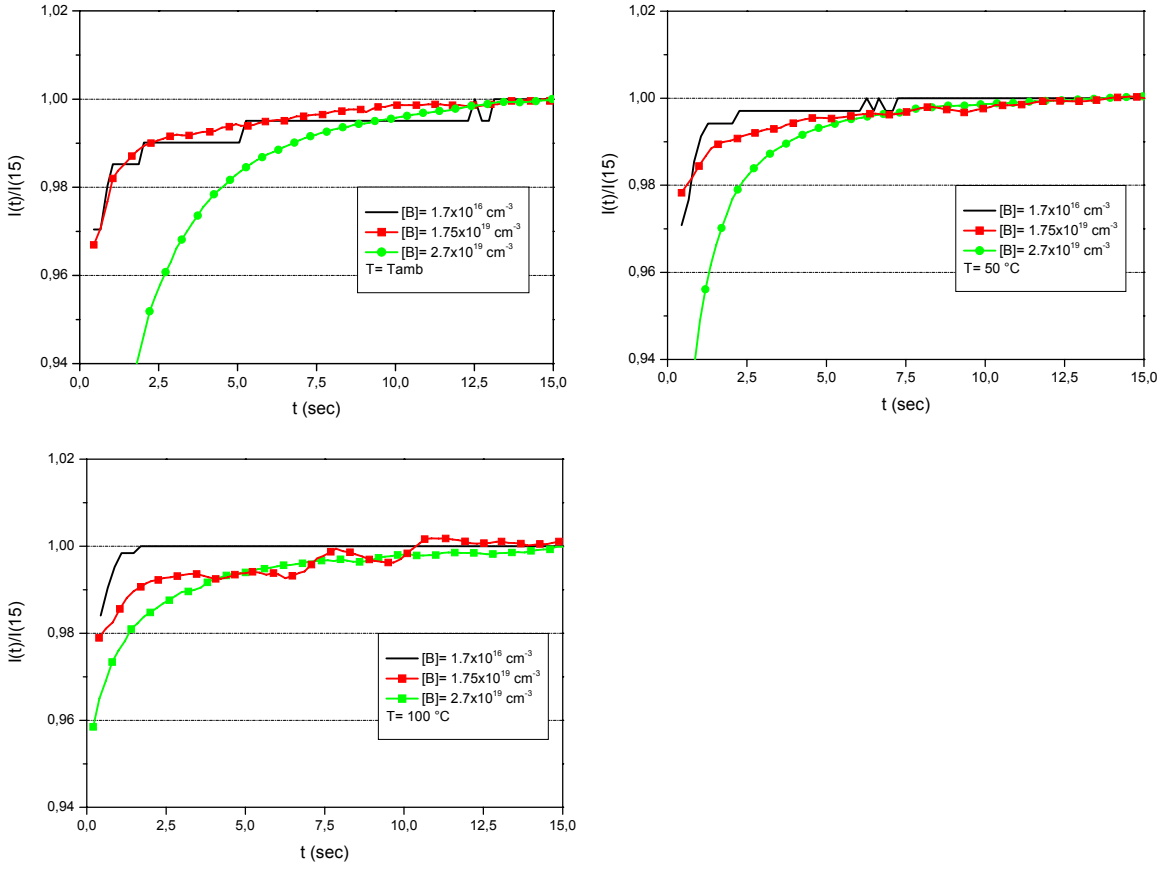

Fig. 6.5 Graphic of time response for three samples and three different doping levels at **(a)** Room temperature, **(b)** 50 °C and **(c)** 100 °C.

As we can see from left to right (at room temperature, 50 °C and 100 °C respectively) the time response diminish with increasing temperature, nevertheless, seems that at room temperature doping level has little effect on time response difference between samples

with doping levels lower than $2x10^{19}$ cm^{-3} that is the limit marked from some researchers [81] as the beginning of the hopping conduction mechanism. In the other hand, this effect becomes more pronounced with increasing temperature where we can see a faster response for the whole set of samples evidenced in a higher gap between different doping levels with respect to the gap found at room temperature, as we said before, time response decrease for decreasing doping levels and increasing temperatures. It is worth noting that the shape of the curves are related to the magnitude of the measured current, which depends on the doping level; in fact at T=100 °C for sample N° 2 we have I= 9 mA; for sample N° 3, I= 1mA and for sample N° 6, I= 0,063 mA. Regarding these effects the first conclusion that we can say is that for an experimental setup apt to be used at high temperatures it is a trend that get us to use samples at low doping level, because of a faster time response.

6.6 EXPERIMENTAL ACQUISITION PAUSE TIME SELECTION

In order to provide the right pause time in experimental acquisition different graphics and conclusions have been take into account. First of all, as we said in chapter 6.5, time response increases for increasing doping level and lower temperatures; as a consequence, we have taken the sample with the highest doping level of the set analyzed (sample N° 2, [B]= $2.7x10^{19}$ cm^{-3}) at room temperature, as the slowest time response able to reach the steady state. Then, with this "worse" condition, we established the time necessary to reach the steady state that becomes the time pause between *I-V* measurements (i.e.: change in the applied voltage through a programmable voltage source in order to build the *I-V* characteristic, see Fig. 6.1(a)). In Fig. 6.2 it is shown the I(t) curve for this sample at room temperature. As we can see from this figure it is clear that after 12 seconds

it is reached a steady state for which we are ready to make the acquisition. However, this is only the threshold for the steady state, because of that we have established a time of 15 seconds as pause time between acquisitions in order to be in a safer condition. This pause time of 15 seconds was used for all *I-V* characteristic that were performed in order to evaluate piezoresistive effect on B-doped p-type CVD diamond films grown at the Mechanical Engineering Department of the University of Rome "Tor Vergata" laboratories.

Chapter 7

Experimental results of piezoresistive measurements

Summary

In this part of the work are presented the investigated electrical and piezoresistive properties of chemical vapor deposited (CVD) boron-doped p-type polycrystalline diamond films grown at the Mechanical Engineering Department of the University of Rome "Tor Vergata" laboratories. The boron-doped p-type diamond films were grown on intrinsic diamond films that act as electrical insulation from silicon substrate, the range of doped film is from 7 μm to 28 μm thickness; separated in a set of six diamond films samples (N° 1, 2, 3, 4, 5 and 6).
In order to characterize the piezoresistive effect, relative change of the electrical resistance $(\Delta R/R_0)$ almost proportional to the applied strain were made; as we will see the "*gauge factor*" (GF) is highly dependent on temperature and doping level.
As it was presented, the focus of the present work and the present measures is to analyze the feasibility of diamond as a high temperature/harsh environment strain gauge material, for which almost all measurements were done reaching high temperatures. Moreover, comparison in temperature and doping level of the sample set are presented in order to evaluate the mentioned dependence.

7.1 INTRODUCTION

In this chapter several measures were done in order to show the behavior of B-doped diamond samples. The first subchapter is intended to explain the temperature dependence of the *I-V* characteristic in order to clarify the key role played in *I-V* measurements, we will see measurements done maintaining constant power at 10 μstrain. After that we will study the relative change of resistance $\Delta R/R$ produced by an applied strain, we will also see little variations in GF as a result of non-ideal linearity between $\Delta R/R$ and the applied strain. The chapter continues analyzing the effect of doping level in the variations of $\Delta R/R$ under strain, conclusions and considerations about doping level and response level will be made, in addition, differences in GF values will be shown in order to clarify and to quantify how doping level affects the response level under strain. At the end of the chapter, in order to test samples in a harsh environments, systematic studies in temperature were made. We will analyze the different response of a set of diamond samples, each one with different doping level, and how they react to the combination of strain and temperature. We will study the relative change of resistance $\Delta R/R$ and GF for the different conditions presented. Conclusion and considerations will be also made in order to enlighten possible diamond growing conditions identifying a material able to be used as a strain gauge apt to operate at high temperatures constituting a harsh environment if we take into consideration the semiconducting nature of diamond and the physical problems derived from temperature.

7.2 TEMPERATURE DEPENDENCE OF I-V CHARACTERISTIC

As it was said in the precedent chapter the I-V characteristic of the diamond samples is the main measure to be done in order to put in evidence the different characteristics of the material such as: Doping level, Gauge factor, $\Delta R/R$. In these measurements temperature plays a key role as it is evidenced in Fig. 7.1 that shows the I-V characteristic of a sample for different temperatures and zero strain level.

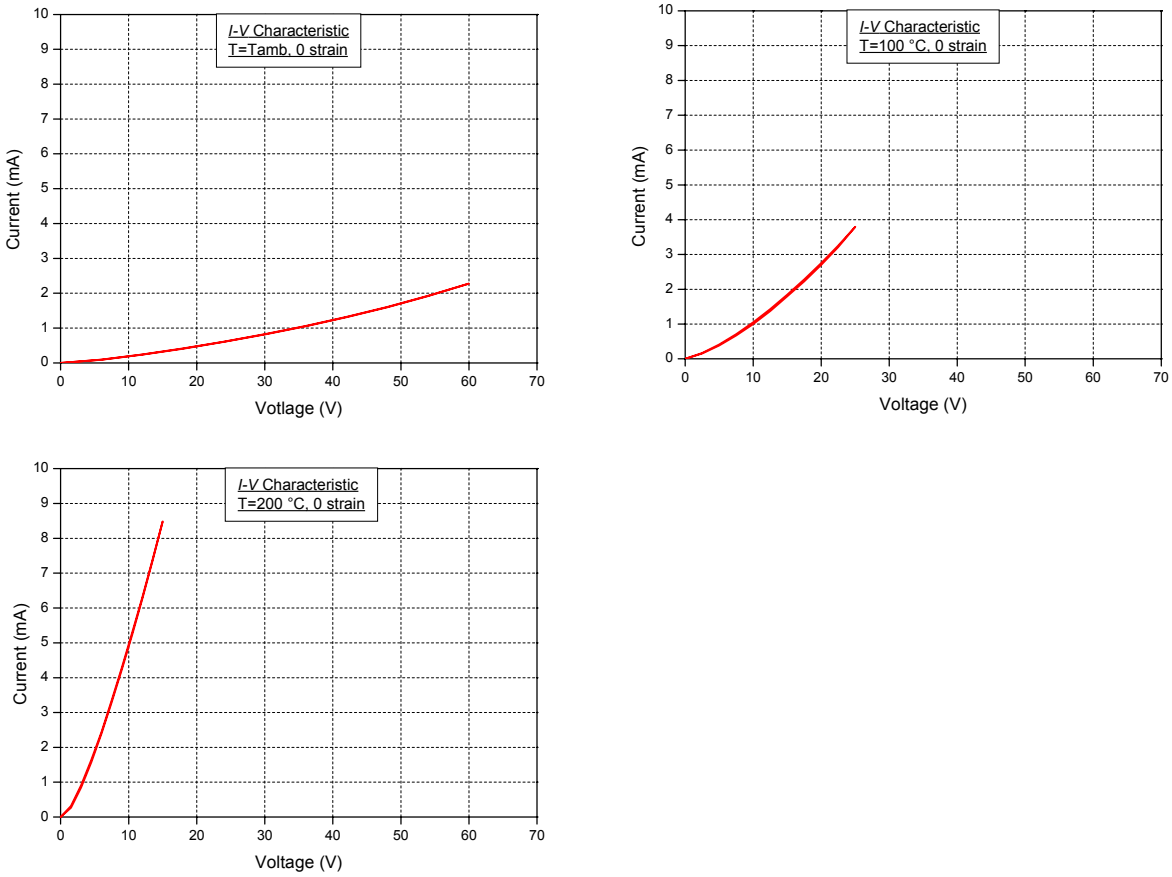

Fig. 7.1 *I-V* characteristic of a diamond sample at **(a)** Room temperature, **(b)** 100 °C and **(c)** 200 °C. It is worth noting the difference in the slope of the curves due to changes in resistivity.

For the three graphics the power area is limited at 700 mW, however in order to limit power dissipation, and to avoid possible structures damages, power was limited to 150 mW approximately ($I \cdot V \leq 150$ mW). As we can see from these figures the lowest value of current occurs at low temperature, then for increasing temperatures current increased as the

resistivity decreased. It is worth noting that linearity only occurs at little power values, thus we cannot say that the *I-V* characteristic of boron-doped p-type diamond films is linear, moreover, we can say that at our power limit the decreasing resistivity is more evident with increasing temperature.

7.3 RELATIVE CHANGE OF RESISTANCE AS A FUNCTION OF APPLIED STRAIN

In this part of the chapter measures of $\Delta R/R$ were made in order to evaluate the relative change of resistance due to an applied strain, thus, the piezoresistive effect (see chapter 4.2). In Fig. 7.2(a) it is shown the mentioned $\Delta R/R$ as a function of the applied strain, the differences in $\Delta R/R$ are measured at the highest voltage value (see Fig 7.2(b)).

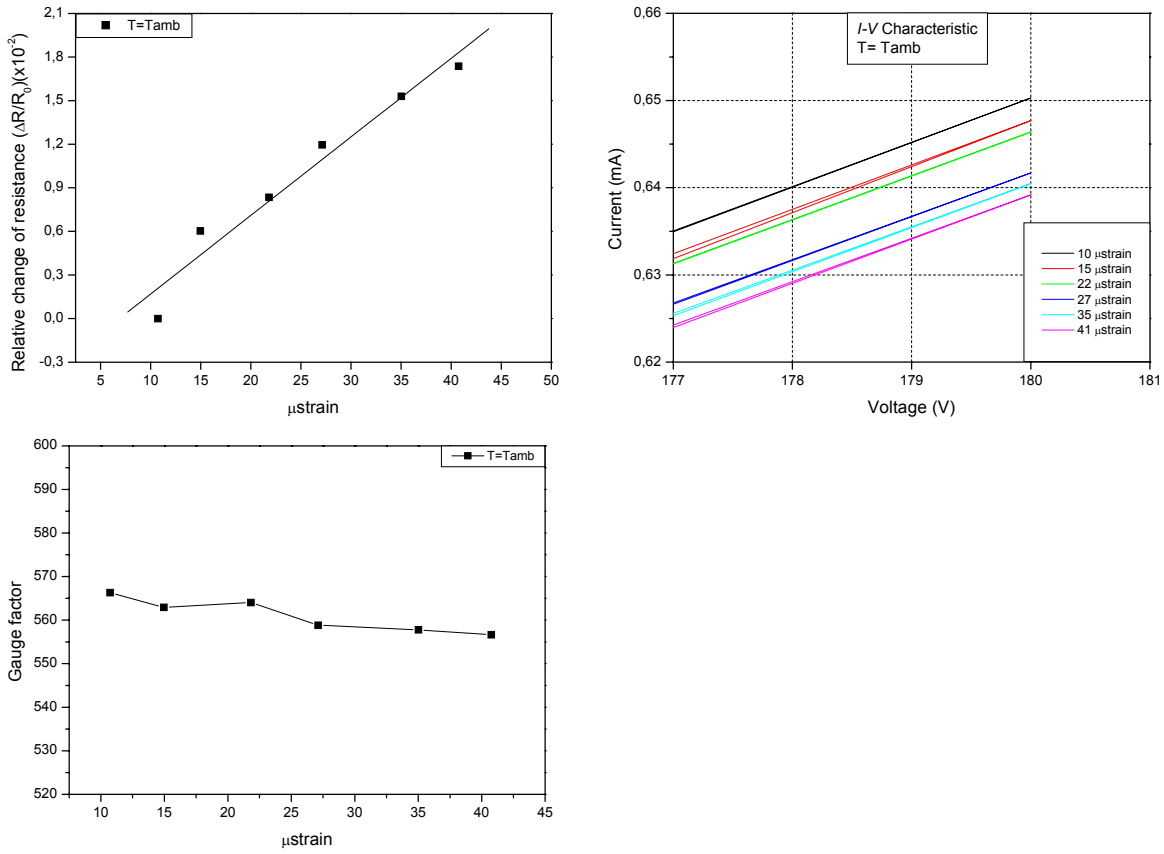

Fig. 7.2 (a) ΔR/R as a function of applied strain, **(b)** Differences in ΔR/R are measured at the highest voltage value and **(c)** Variations of "*gauge factor*" with applied strain.

Where R and R_0 are the electrical resistances at strain different from zero (>10 μstrain) and 10 μstrain respectively and $\Delta R = R - R_0$. In Fig. 7.2(c) the behavior of the GF with applied strain is shown, it is evidenced a little decrease in GF with increasing strain, this simple behavior could be explained by the formula used to calculate GF and it is shown in Eq. 4.13, the strain value *(ε)* was calculated by Eq. 5.1, thus, the little decrease in GF corresponds to a non-ideal linear behavior of the relative change in resistance with strain, which is clearly shown in Fig. 7.2(a).

7.4 RELATIVE CHANGE OF RESISTANCE AS A FUNCTION OF DOPING LEVEL

As it is well known there is a relation between the relative change of resistance of a diamond sample, subjected to an applied strain, and the doping level [73]; in order to evaluate this effect, systematic measurements were done. In Fig. 7.3 are shown different curves for different doping level samples at room temperature.

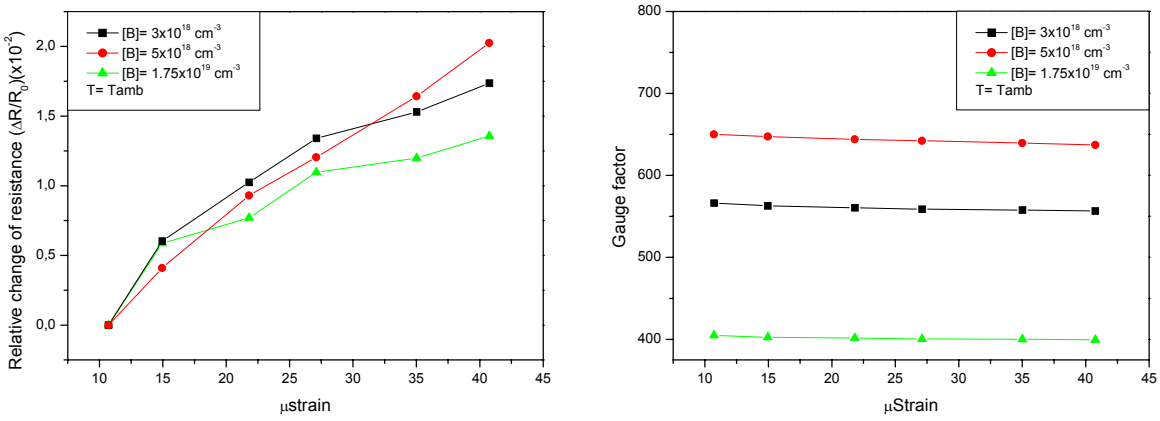

Fig. 7.3 Characterization of three different samples with different doping levels **(a)** ΔR/R as a function of applied strain and **(b)** Gauge factor as a function of applied strain.

As we can see in Fig. 7.3(a) relative change of resistance decreases with decreasing resistivity, then, in Fig. 7.3(b) we can see that the gauge factor follows the same trend. This different behavior of the diamond samples could be explained because it is believed that different doping level, responsible for the creation of acceptor levels, modifies the band structure in order to react with the applied stress in different way, depending on the doping level (see chapter 4.2). The gauge factor for these samples and the strain were calculated using Eqs. (4.13) and (5.1). The effect of transverse strain was neglected. It is worth noting that in Fig. 7.2(b) the gauge factor reaches values as high as 650 at room temperature; this fact tells us that diamond is not only a suitable material for working at high temperatures / harsh environments but also a suitable material to be used in standard (low temperatures) applications; as a counterpart diamond is an inert material to almost all chemical attack which in this case could present serious problems to the microelaboration in order to produce electronic devices; nevertheless, disadvantages at low temperature and standard applications become the main outstanding properties of diamond apt to be used in aggressive environments.

7.5 STUDY OF PIEZORESISTIVE PROPERTIES OF PECVD P-DOPED DIAMOND AT HIGH TEMPERATURES

In this part of the chapter we introduce the concept of the use of diamond as a potential material to be used in hostile environments; in this particular case, temperature acts as harsh environment. In order to analyze piezoresistive properties at high temperature, comparisons of $\Delta R/R$ for sample Nº 5 as a function of temperature were made. Moreover, GF as a function of strain and temperature will be analyzed.

Because of its wide bandgap (5.35 eV) diamond is an outstanding material apt to work at high temperatures because of its transport properties under conditions where silicon is saturated and lose any property as semiconductor device. As we can see in Eq. (3.1) conductivity increases by an exponential relation with temperature, these are the conduction mechanisms that govern the carrier transport in diamond and its macroscopically properties. The high bandgap of diamond allows to have a material able to be used, and measure his properties, at high temperatures. For that reason measurements of GF and $\Delta R/R$ at high temperature (till 200 °C) were performed.

In Fig. 7.4 it is shown the graphic of relative change of resistance $\Delta R/R$ as a function of the applied strain and temperature, this graphic shows some scattering but is evident a trend in which $\Delta R/R$ decreases for increasing temperatures, in accordance with literature and experiments from others research groups [72].

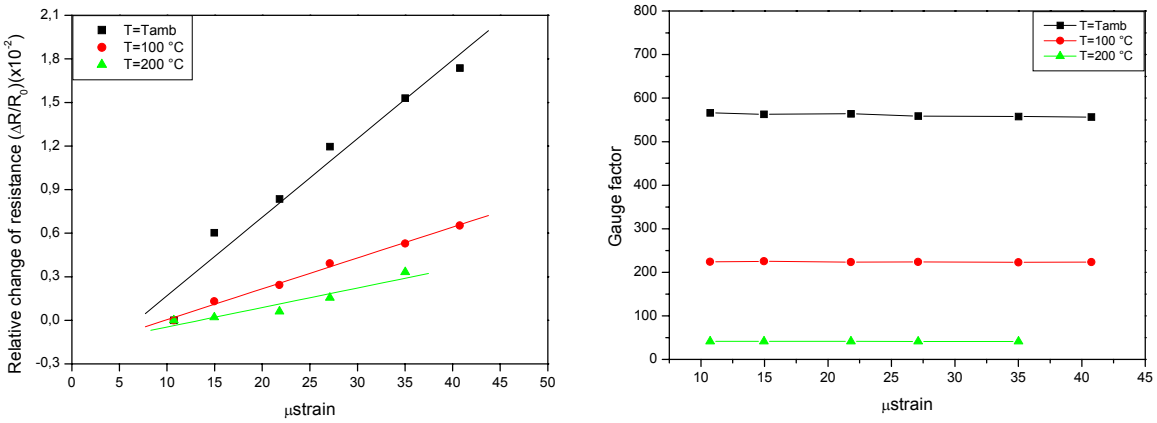

Fig. 7.4 (a) Temperature dependence of ΔR/R with applied strain for three different temperatures and **(b)** Temperature dependence of "*gauge factor*" with applied strain for three different temperatures.

In this graphic is also shown the little change of the GF depending on the applied strain (see Fig. 7.4(b)). It is worth noting that little change in GF correspond to little change in applied strain. Fig. 7.5 shows the GF for a diamond sample (Nº 5) as a function of temperature and it clearly shows the temperature dependence of the "*gauge factor*" (GF)

that can be fitted by an exponential function, as it was said before, this behavior has a direct correlation with the relative resistance change of the sample for different temperatures.

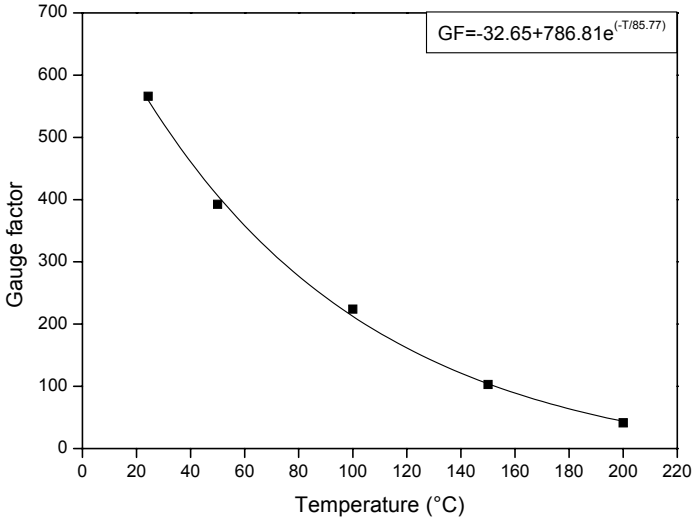

Fig. 7.5 Temperature dependence of the "*gauge factor*" for a diamond sample (N° 5).

The above mentioned dependence of the relative change in resistance with temperature it is clearly shown in Fig. 7.6, in which, we have the comparison of three different samples: N° 3, N° 4 and N° 5, with three different doping levels 1.75×10^{19} cm^{-3}, 5×10^{18} cm^{-3} and 3×10^{18} cm^{-3} respectively. In each individual graphic it is observed how doping level affects the $\Delta R/R$ response and then GF; it is shown that $\Delta R/R$ response diminish with increasing doping level. If the three graphics are observed simultaneously from left to right we can see that curves flatten as a function of increasing temperature. As it was said before a proper explanation of the mechanisms that govern the carrier transport in diamond and its macroscopic properties could be find in chapter 3.

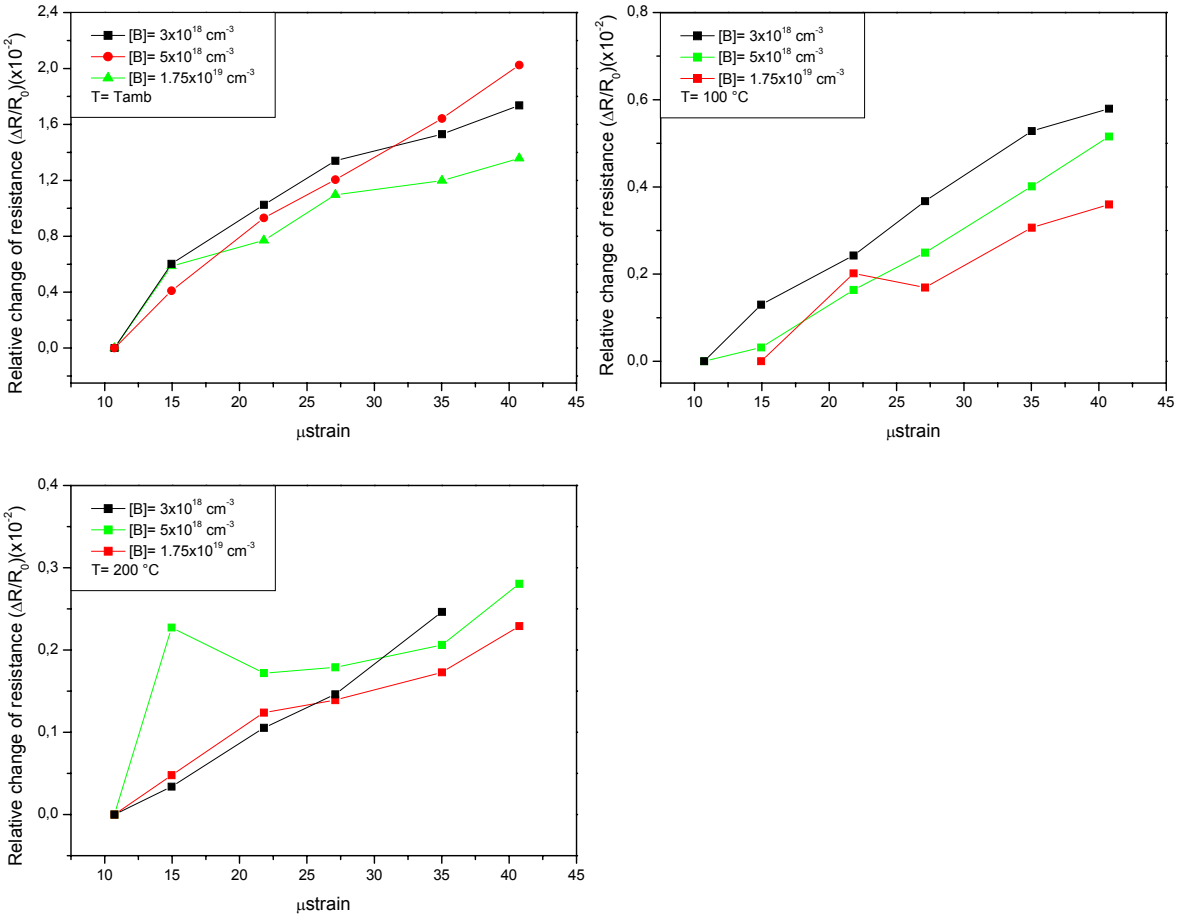

Fig 7.6 ΔR/R as a function of applied strain for three different doping levels at **(a)** Room temperature, **(b)** 100 °C and **(c)** 200 °C.

Regarding how $\Delta R/R$ is affected in Fig 7.6 we can observe what happens to GF. It is shown that $\Delta R/R$ response diminishes with increasing doping level, the same behavior it's observed for GF in Fig. 7.7. At room temperature GF of the diamond samples were about 600 for the sample of lower doping level and remain above 70 even at 200 °C; the results shows that B-doped CVD diamond films are potentially useful materials for piezoresistors apt to be used at high temperature. Regarding on GF, which is the main factor to be used for harsh environment design, we can see that even at high temperatures diamond shows piezoresistive properties that make diamond an unique material apt to sense pressure at high temperature.

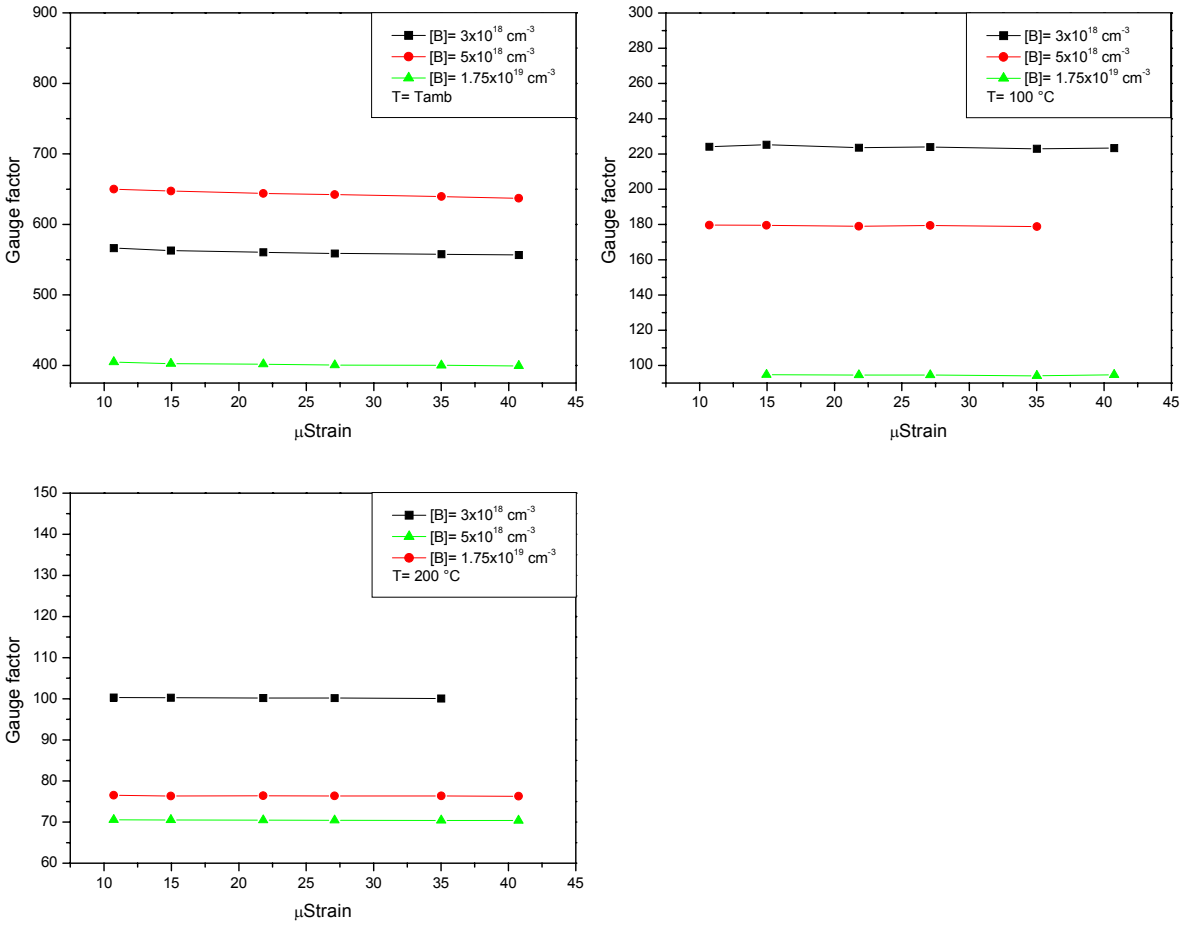

Fig. 7.7 "*Gauge factor*" as a function of applied strain for three different doping levels at **(a)** Room temperature, **(b)** 100 °C and **(c)** 200 °C.

In Fig. 7.8 we can observe the GF behavior of the same set of samples previously analyzed as a function of temperature for their different doping levels and for 10 μstrain.

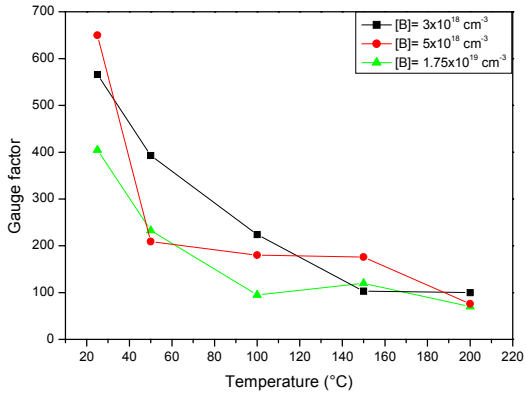

Fig. 7.8 "*Gauge factor*" of the set of samples previously analyzed as a function of temperature.

In this figure we can appreciate the decreasing value of GF as temperature and doping level increase, however we cannot see relevant differences. For that reason let's take into account other two samples, one with higher doping level than those analyzed before and the other one with lower doping level than those analyzed before. In particular, two samples with a doping level of $1.7x10^{16}$ cm^{-3} and $6x10^{19}$ cm^{-3} respectively will be included, moreover, we will compare them with a diamond sample belonging to the previous group, the chosen sample was that showing a doping level of $1.75x10^{19}$ cm^{-3}; in Fig. 7.9 we can see the comparison of this three samples.

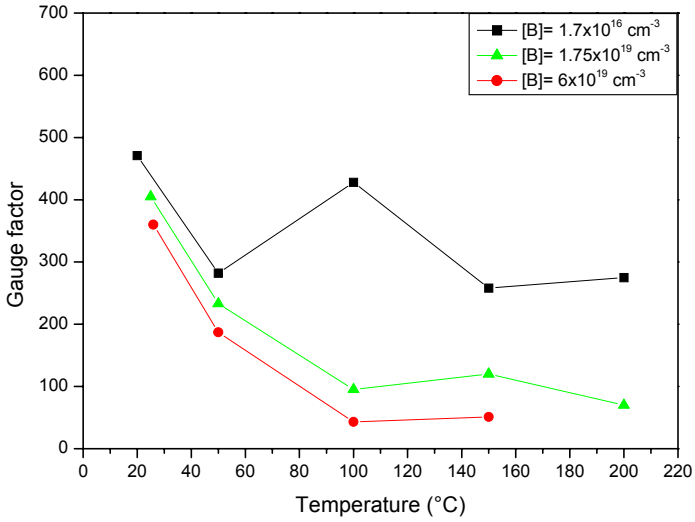

Fig. 7.9 "*Gauge factor*" of a set of samples, with extreme doping level values, as a function of temperature.

As we can see in this figure, there is a remarkable difference between diamond samples with relevant differences in doping level. This fact could enlighten which type of doping level could be necessary in a "potential" application of CVD P-doped diamond as a strain gauge, because, a higher doping level could worsen the response of the device with temperature. In the other hand, a trade off must be done in order to evaluate higher Johnson noise level due to a higher resistivity level.

In Tab. 7.1 is resumed the values of Fig. 7.8 and 7.9, this table is sort by increasing doping level in which we can see a trend in increasing GF as a function of decreasing doping level and decreasing temperature.

Table 7.1 Resuming table of main characteristic of the set of samples used for piezoresistive effect measurements.

Sample	N° 1	N° 3	N° 4	N° 5	N° 6
Doping level (cm^{-3})	$6x10^{19}$	$1.75x10^{19}$	$5x10^{18}$	$3x10^{18}$	$1.7x10^{16}$
GF (25 °C)	360	405	650	566	471
GF (50 °C)	187	233	209	393	282
GF (100 °C)	43	95	180	224	428
GF (150 °C)	51	120	176	103	258
GF (200 °C)	-	70	76	100	275

It is worth noting that even at 200 °C GF remains higher than 250 for sample Nº 6, this is an important result in order to project high temperature devices because it is clear that devices that have to work at high temperatures must have little doping levels in order to read an important signal under pressure action.

CONCLUSIONS

The present PhD thesis was focused on growing, doping, characterization and testing of Boron-doped p-type diamond films. This work was developed at the Mechanical Engineering Department of the University of Rome "Tor Vergata" laboratories. Due to its high energy gap between valence band and conduction band (apt to operate at high temperatures) and other remarkable electronic, chemical, physical and mechanical properties such as, high melting point, low chemical reactivity and extreme robustness, diamond seems to be a natural candidate for the realization of microsystems apt to operate in harsh/hard environments.

In particular, in the first step of the PhD period work was focused in the growth of intrinsic diamond on silicon substrates in order to growing the insulator diamond layer. After that, work was addressed to diamond doping, by means of, a solution of solid boron oxide (B_2O_3) in methanol (CH_3OH) was used as doping agent; this solution was introduced into the growth chamber in order to grow boron-doped p-type thin diamond films on the previous intrinsic diamond films. Later in the PhD period, systematic studies were performed in order to understand the growth chamber dynamics; two main kind of growing strategies were used, the so called: "*Doped at once and growing systematic study"* and the so called "*Doped at once and growing in presence of methanol systematic study"*, the first one was intended to make a first sample growth with the mentioned doping solution and make successive growths without any doping agent but the contamination of the chamber as doping agent. Then, the second systematic study was intended to study the inhibitor behavior that the presence of methanol has in the growth chamber; conclusions and considerations were made in order to bring some light over growth chamber dynamics.

Once boron-doped diamond samples were grown, a characterization of the electrical properties derived from doping were performed, for that, resistance as function of temperature experiments were done, the so called: R(T). It is worth noting that conclusions on chamber dynamics were made studying their R(T) behavior. Knowing the growth chamber dynamics it was possible to have some level of control of the parameters involved in boron doping growth, then, it was possible to classify diamond samples through its boron content. Moreover, it was possible to calculate the energy of the acceptor level for any single boron-doped diamond sample, known as activation energy "E_a", i.e.: the acceptor level is the energy necessary to move an electron from the valence band to an acceptor state in the forbidden gap, thus, generating a vacancy in valence band and by this way hole conduction. R(T) measurements was also useful to calculate the *Temperature Coefficient of Resistance* (TCR), we found that TCR is strongly dependent on doping level, in the range of room temperature – 200 °C we calculate a TCR from 22000 ppm/°C to 10000 ppm/°C arriving to a value of 1000 ppm/°C for the highest doped samples at 450 °C; know this parameter it is important due to its capability of hiding piezoresistive effect, so in order to avoid this undesirable effect an accurate control of temperature was established.

Following this work the reader will find an introduction of some parameters that must be taken into account regarding microsensors, such as: Sensor response curve, internal sensitivity, resolution, noise and drift. Always in the same chapter a description of the band theory of piezoresistive effect and its numerical approach is presented; later, some opportunities where diamond could be an useful material apt to be used in diamond-based sensors are described.

In the fifth chapter the experimental setup for the piezoresistive effect demonstrator is presented; it is described the force application system and its calibration, the thermal

regulation and the data acquisition system in order to perform the *I-V* characteristic of the different boron-doped diamond films.

As the reader could appreciate in this work an important parameter that has been into account is the time response of diamond films. Through *I-V* measurements it was possible to manifest and to quantify the mentioned effect; nevertheless, the *I-V* characteristic showed that there is an "apparent" hysteresis effect when voltage was varied, it means, there is a gap between increasing and decreasing applied voltage that conditioned the data acquisition pause necessary to reach the steady state in current; for that, different studies were made in order to take into account all the different variables that take part in established the data acquisition pause. The effect of temperature was analyzed, we found that time response decrease with increasing temperature. A proper explanation could be found through the change of resistivity with temperature, in which the effective mass (m*) is taken as a parameter that depends on temperature [79], that causes changes in the carriers number [80] which is macroscopically verified by the change in the time response. The variation of time response with applied strain was also studied, we found that time response diminishes with increasing applied strain. The explanation of this phenomenon could be approached in the following direction, the strain that made changes in the heavy hole and light hole bands (degenerated from the valence band, see chapter 4.2) causes changes in the carriers type involved in electrical conduction [61], thus difference in the resistivity that is verified by means of different time response from CVD diamond samples with different applied strain levels. The work was also addressed to study the combined effect of doping level and temperature in order to enlighten possible growth conditions able to be used in a diamond-based strain gauge and the variables that could take part in its utilization in harsh environments; we found that at room temperature little differences are verified for diamond samples with doping level lower than $2x10^{19}$ cm^{-3}, that is the

threshold marked for some researchers as the beginning of the hopping conduction mechanism [81], however, at higher temperatures (50 °C and 100 °C) it is verified that time response diminishes with decreasing doping level. The previous mentioned effects of temperature, strain and doping level in time response lead us to established a pause acquisition time of 15 seconds, this pause time was used in all *I-V* characteristic made in order to study piezoresistive effect on diamond thin films samples.

At this point of the work, experimental measurements were performed in order to evaluate piezoresistive effect to qualify and quantify diamond as a strain gauge. In particular, temperature dependence of the *I-V* characteristic was analyzed for a fixed power of 100 mW, because of the change in resistivity with temperature it is clear that *I-V* characteristic was modified increasing its current (decreasing voltage applied) for the same power value. Later, it was analyzed the strain response at room temperature, for that, measurements of the relative change of resistance $\Delta R/R$ were made; it was observed that for tensile strain a relative, almost linear, positive change in resistance was verified; *gauge factor* "GF" was also calculated by Eq. 4.13, little decrease in GF was verified corresponding to a non-ideal linear behavior of the relative change in resistance with strain, which is clearly shown in Fig. 7.2(a). Besides this, systematic studies of the relative change of resistance $\Delta R/R$ as a function of doping level at room temperature were done; results show that with increasing doping level there is a worsening in $\Delta R/R$, it means, the curves flatten as increasing doping level, as a consequence GF diminishes, then, there is a sensible worsening in GF response. In order to have a complete analysis, combined effects of temperature, doping level and strain were analyzed, the results show that piezoresistive response is highly dependent on temperature and doping level, it means, in order to evaluate piezoresistive effect an accurate control of temperature must be done, if not, there is a risk of hiding the mentioned effect; nevertheless, we can conclude that low doping

level is the trend to build a diamond based strain gauge; as it was said before, low levels of doping give higher $\Delta R/R$ and GF response, then, a higher signal level that better shows piezoresistive effect; this fact it is evidenced with sample Nº 5 with a doping level as low as 1.7×10^{16} cm^{-3} for which GF remains higher than 250 even at 200 °C. We hope this work brings light to future developments in order to build a diamond-based strain gauge; to this purpose there is in course a collaboration with Gefran Sensori Spa which is the industrial partner in charge of the technology transfer in order to obtain a real device apt to take advantage of the unique properties of diamond to be used in harsh/hard environments.

Bibliography

[1] I. Fujimasa, *Micromachines, a new era in mechanical engineering*. Oxord University Press (1996).

[2] I.J. Busch-Vishniac, *Electormechanical sensors and actuators*. Dekken Inc. (1998).

[3] K. Tsuruta, Y. Mikuriya, Y. Ishikawa, *Microsensor development in Japan*. Sensor Review 19 (1999) 37-42.

[4] H. Fujita, *Microactuators and micromachines*. IEEE Proc. Vol. 86, n.8 (1998) 1721-1732.

[5] D.S. Eddy, D.R. Sparks, *Applications of MEMS technology in automotive sensors and actuators*, Proc. of the IEEE, Vol.86, n.8 (1998) 1747-1754.

[6] N.Maluf, *An introduction to Microelectromechanical systems engineering*. Artech House publishers, Boston (2000).

[7] K.E. Petersen, *Silicon as a mechanical material*. IEEE Proc. Vol. 70, n.5 (1982) 420-457.

[8] I. Brodie, J.J. Murray, *The physics of Microfabrication*. New York, NY: Plenum Publ. (1982).

[9] P. Sigmund, *Sputtering by Particle Bombardment I*. Ed. R. Behrish, Topics in Applied Physics, Vol. 47 (1981).

[10] P.D. Towsend, *Sputtering by Particle Bombardment II*. Ed. R. Behrish, Topics in Applied Physics, Vol. 47 (1982).

[11] A.J. Steckl, *Particle-beam fabrication and in situ processing of integrated circuits*. IEEE Proc. Vol. 74, n.12 (1986) 1753-1774.

[12] F. Cerrina, *Application of X-rays to nanolithography*. IEEE Proc. Vol. 84, n.4 (1997) 644-651.

[13] F. Cerrina, *X-ray Lithography*. SPIE Handbook on Lithography (1997).

[14] G.T.A. Kovacs, N.I. Maluf, K.E. Petersen, *Bulk micromachining of Silicon*. IEEE Proc. Vol. 86, n.8 (1998) 1536-1551.

[15] J.W. Coburn, H.F. Winters, *Plasma etching-A discussion of mechanism*. J. Vac. Sci. Technol. Vol. 16, n.2 (1979) 391-403.

[16] D. Basting, H. Endert, *Excimer lasers for industrial microprocessing*. The Industrial Physicist, American Institute of Physics Publ. (1997) 40-44.

[17] H. Guckel, *High-aspect-ratio micromachining via deep X-ray lithography*. IEEE Proc. Vol. 86, n.8 (1998) 1586-1593.

[18] K. Ikuta, K. Hirovatari, *Real three dimensional fabricating using stereo lithography and metal molding*, IEEE Proc. Vol. 2, n.3 (1993).

[19] A.M. Stoneham, *Recent development in the theory of diamond*.
The properties of diamond, Ed. J.E: Field, Academic Press (1990) 185

[20] C. Bauer et al., *Radiation hardness studies of CVD diamond detectors*.
Nucl. Instr. Meth. in Phys. Res. A 367 (1995) 207.

[21] C.A. Klein, G.F. Cardinale.
Diamond and Related Material 2 (1993) 918.

[22] M. Werner, R. Locher, *Growth and application of undoped and doped diamond films*.
Rep. Prog. Phys. 61 (1998) 1665.

[23] W.L. Wang, X. Jiang, K. Taube, C.P. Klages.
J. Appl. Phys. 82 (2) (1997) 729.

[24] I. Taher, M. Aslam, M.A. Tamor, T.J. Potter, R.C. Elder.
Sensors and Actuators A 45 (1994) 45.

[25] J.R. Olson, R.O. Pohl, J.W. Vandersande, A. Zoltan, T.R. Antony, W.F. Banholzer.
Phys. Rev. B 47 (1993) 14850.

[26] J.I. Pankove, C.H. Qiu, *Optical properties and optoelectronic application of diamond*, Syntetic Diamond, Ed. K.E. Spear and J. P. Dismukes, Wiley and Son Publ. (1994).

[27] J.C. Angus, *Structure and thermochemistry of diamond*.
The Physics of Diamond, Ed. A. Paoletti, A. Tucciarone, IOS Press (1997) 9-30.

[28] R.J. Weldake, *Technology of Diamond Growth*.
The properties of Diamond, Ed. J.E. Field, Academic Press (1990) 501.

[29] B.V. Derianguin, D.V. Fedoseev, V.M. Lukyanovich, B.V. Spitzin, V.A. Ryabov, A. Lavrentyev, J. Crist. Growth 2 (1968) 380.

[30] B.V. Derianguin, D.V. Fedoseev.
Carbon, 11 (1973) 299.

[31] X. Jiang, C.P. Klages.
Diam. Relat. Mater. 2 (1993) 1112.

[32] C.A. Wolsen, Z. Sitar, R.F. Davis, *Combustion Flame Deposition of Diamond*.
Low Pressure Synthetic Diamond, Ed. B. Dischler, C. Wild Spring (1988) 41.

[33] S. Matsumoto, Y. Sato, M. Kamo, N. Seneka.
Japan J. Appl. Phys. 21L (1982) 183.

[34] M.A. Cappelli, T.G. Owano, *Plasma-Jet Deposition of Diamond*.
Low Pressure Synthetic Diamond, Ed. B. Dischler, C. Wild Spring (1988) 59.

[35] P.K. Bachamann, *Plasma Chemical Vapour Deposition of Diamond Films*.
The Physics of Diamond, Ed. A. Paoletti, A. Tucciarone, IOS Press (1997) 45-71.

[36] G. Balestrino, M. Marinelli, E. Milani, A. Paoletti, I. Pinter, A. Tebano.
Appl. Phys. Let. 62 (8) (1993) 879.

[37] G. Balestrino, M. Marinelli, A. Tebano, A. Paoletti, G. Luce, I. Pinter,
B. Antonini, P. Paroli, Vuoto, 22 (1992) 5.

[38] G. Verona Rinati, *Applicazioni del diamante sintetico nella tecnologia dei microsistemi*, Tesi di Dottorato, Univ. Roma "Tor Vergata" (1999).

[39] E. Hyman, K. Tsang, A. Drobot, B. Lane, J. Casey, R. Post.
J. Vac. Sci. Techn. A 12 (1994) 1474.

[40] B.V. Deryagin, D.V. Fedoseev, *Growth of diamond and graphite from the gas phase*.
Surf. Coat. Technol. 38 (1989) 131.

[41] D.G. Goodwin, J.E. Butler, *Theory of diamond chemical vapour deposition*.
Handbook of Ind. Diam. and Diam. Films, Ed. M. Prelas, G. Popovici, L. Bigelov.

[42] P.K. Bachmann, D. Leers, H. Lydtin, D.U. Wiechert.
Diamond Relat. Mater. 1 (1991) 1.

[43] M. Marinelli, E. Milani, M. Montuori, A. Paoletti, P. Paroli.
Appl. Phys. Lett. 65 (22) (1994) 2839.

[44] M. Angelone, *Sviluppo ed applicazione di microsensori di diamante CVD per misure nucleari in ambienti ostili*, Tesi di Dottorato, Univ. Roma "Tor Vergata" (2002).

[45] M. Marinelli, E. Milani, A. Paoletti, A. Tucciarone, G. Verona Rinati,
M. Angelone, M. Pillon, Appl. Phys. Lett. 75 (1999) 3216.

[46] M. Werner, O. Dorsch, E. Obermeier.
Electron Technol. 27 (1994) 83.

[47] M. Werner, *Low Pressure Synthetic Diamond: Manufacturing and Applications*.
Ed. B. Dischler and C. Wild (Berlin : Springer) 243.

[48] M. Werner, O. Dorsch, E. Obermeier.
Diam. Relat. Mater. 4 (1995) 873.

[49] A.J. Tessmer, L.S. Plano, D.L. Dreifus.
IEEE Electron. Devices Lett. 14 (1993) 66.

[50] P. Gluche, A. Aleksov, A. Vescan, W. Ebert, E. Kohn.
IEEE Trans. Electron. Devices Lett. 18 (1997) 547.

[51] M. Masood, M. Aslam, M. A. Tamor, T. J. Potter.
Appl. Phys. Lett. 61 (1992) 1832.

[52] M. Aslam, G. S. Yang, A. Masood.
Sensor and Actuators A 45 (1994) 131.

[53] M. Werner, O. Dorsch, E. Obermeir.
Diam. Relat. Mater. 4 (1995) 873.

[54] M. N. Gamo, I. Sakaguchi, E. Yasu, K. Ushizawa, H. Haneda, T. Ando.
10th Conference on Diamond and Related Materials Procedings.

[55] A. T. Collins and E. C. Lightowlers, *Electrical properties*.
The properties of Diamond, Ed. J.E. Field, Academic Press (1990) 92.

[56] N. F. Mott and E. A. Davis.
Philos. Mag. 17 (1968) 1269 – 1284.

[57] Charles Kittel.
Introduction to Solid State Physics, J. W and Sons Inc, 7th ed. (1996) 231.

[58] R. Erz, W. Dötter, K. Jung, H. Ehrhardt, *Investigation of boron and hydrogen concentrations in p-type diamond films by infrared spectroscopy*. Diam. Relat. Mater. 4 (1995) 469-472.

[59] A. D'Amico, C. Di Natale. *A Contribution on Some Basic Definitions of Sensors Properties*. IEEE Sensors Journal, Vol. 1, N° 3, October 2001.

[60] C. J. Rauch, *Millimeter cyclotron resonance in diamond*.
Proc. Int. Conf. Semiconduct. Phys., 1962, Institute of Physics and Physical Society, London, 1962, 276.

[61] V. K. Bazhenov, I. M. Vikulin and A. G. Gontar, *Synthetic diamonds in electronics (review)*. Sov. Phys. Semicond., 19 (1985) 829.

[62] W. P. Mason and R. N. Thurston, *Use of piezoresistive materials in the measurement of displacement, force and torque*, J. Acoust. Soc. Am., 29 (1957) 1096-1101.

[63] W. P. Mason, *Semiconductor transducers – general considerations*, in W. P. Mason (ed.), Physical Acoustics, Vol. 1, Academic Press, New York, 1964, p. 173.

[64] R. N. Thurston, *Use of semiconductor transducers in measuring strain, accelerations and displacements*, in Physical Acoustics, Vol. 1, Academic Press, New York, 1964, p.215.

[65] C. S. Smith, *Piezoresistance effect in germanium and silicon*. Phys. Rev., 94 (1) (1954) 42-49.

[66] H. J. McSkimin, P. A. Jr and P. Glynn, *The elastic stiffness moduli of diamond*. J. Appl. Phys., 43 (1972) 985-987.

[67] C. A. Klein and G. F. Cardinale, *Young's modulus and Poisson's ratio of "CVD" diamond*, Diamond and Related Mater., 2 (1993) 918-923.

[68] M. Werner, S. Hein and E. Obermeier, *Elastic properties of thin polycrystalline diamond films*, Diamond and Related Mater., 2 (1993) 939-942.

[69] J. C. Erskine, *Polycrystalline silicon-on-metal strain gauge transducers*. IEEE Trans. Electron Dev., ED-30 (1983) 796-801.

[70] P. J. French, *Piezoresistance in polysilicon*. Electron. Lett., 24 (1984) 999-1000.

[71] P. J. French and A. G. R. Evans, *Polycrystalline silicon strain sensors*. Tech. Digest, 3rd Int. Conf. Solid-State Sensors and Actuators (Transducers '85), Philadelphia, PA, USA, June 11-15 1985, pp. 281-283.

[72] M. Deguchi. M. Kitabatake and T. Hirao, *Piezoresistive properties of CVD p-type diamond strain gauges fabricated on diaphragm structure*. Diam. Relat. Mater. 5 (1996) 728-731.

[73] J. L. Davidson, D. R. Wur, W. P. Kang, D. L. Kinser and D. V. Kerns. *Polycrystalline diamond pressure microsensor*. Diam. Relat. Mater. 5 (1996) 86-92.

[74] E. Kohn, P. Gluche and M. Adamschik, *Diamond MEMS – a new emerging technology*. Diam. Relat. Mater. 8 (1999) 934-940.

[75] P. Gluche, M. Adamschik, A. Vescan, W. Ebert, F. Szücs, H. J. Fecht, A. Flöter, R. Zachai and E. Kohn. Diam. Relat. Mater. 7 (1998) 779-782.

[76] A. Flöter, H. Güttler, G. Schulz, D. Steinbach, C. Lutz-Elsner, R. Zachai, A. Bergmaier and G. A. Dollinger. Diam. Relat. Mater. 7 (2-5) (1998) 283-288.

[77] M. Werner, S. Klose, F. Szücs, Ch. Moelle, H. J. Fecht, C. Jhonston, P. R. Chalker, I. M. Buckley-Golder. Diam. Relat. Mater. 6 (1997) 344-347.

[78] M. Mehregany, and S. Roy, *Introduction to MEMS*. 2000, Microengineering Aerospace Systems, El Segundo, CA, Aerospace Press, AIAA, Inc., 1999.

[79] A. T. Collins and E. C. Lightowlers, *Electrical properties*. The properties of Diamond, Ed. J.E. Field, Academic Press (1990) 84.

[80] A. T. Collins and E. C. Lightowlers, *Electrical properties*.
The properties of Diamond, Ed. J.E. Field, Academic Press (1990) 81.

[81] J. P. Lagrange, A. Deneuville and E. Gheeraert, *A large range of boron doping with low compensation ratio for homoepitaxial diamond films*. Carbon 37 (1999) 807-810.